Artefacts associated with electrical measurements of the rock matrix formation factor - response to the request by SSM for supplementary information on retention of radionuclides (SSM2011-2426-110)

Martin Löfgren – Niressa AB

2014-01-29

Contents

1 Introduction

This report is a response to a request for supplementary information (SSM 2013) made by the Swedish Radiation Safety Authority, SSM. The report deals with artefacts that may be induced when estimating the rock matrix formation factor by using electrical methods. The formation factor F_f (–) can be seen as a property factor of the rock matrix's microporous system that is of importance for solute exchange between the rock matrix and freely flowing groundwater in fractures. Formation factors have been used for estimating the effective diffusivity D_e (m^2/s) of radionuclides and groundwater constituents, and have in this way been included in the safety assessment SR-Site (cf. SKB 2010a, Section 6.8). The relation between the effective diffusivity and formation factor is given by:

$$D_e = D_w \cdot F_f \qquad \text{Equation 1}$$

where D_w (m^2/s) is the diffusivity of the solute in free, unconstrained solution. Electrical methods have been used for many decades when estimating the formation factor, both in the laboratory and in situ (e.g. Archie 1942). The in situ electrical methods have traditionally been used in much more porous rock than that commonly found at the Forsmark site, predominantly in prospecting for oil, but sometimes also for minerals. Accordingly, the wide knowledgebase existing is not always transferable to the conditions of interest for a KBS-3 repository. On the other hand, measuring the formation factor by electrical methods in the laboratory is a quite established method, also for dense rock (e.g. Skagius and Neretnieks 1983). SKB has relatively recently adapted these methods to be used in situ in the site investigations, to be able to investigate the undisturbed rock mass at the in situ stress. However, no such measurement has been performed by other national programmes within the field of radioactive waste management. Accordingly, SKB is obligated to defend in detail the usage of data from such measurements in the safety assessment SR-Site, as well as describing artefacts that the method may bring about.

If the in situ electrical method would have given comparable values as the traditional laboratory diffusion measurements, it is conceivable that its data would only have been used in a supporting role in the safety assessment. The rationale would have been that the method lacks in maturity, and is not used by other major parties within the scientific community. However, the in situ electrical method clearly indicates that laboratory measurements overestimate the rock matrix formation factor in a way that would be non-conservative for a safety assessment, with respect to radionuclide retention. Accordingly, such data cannot be disregarded. Moreover, there are concerns that there remain a few artefacts for the electrical methods that are not corrected for. If being properly corrected for, they may bring about even lower formation factors than estimated so far. Such artefacts are discussed in this report.

It is envisaged that other national programmes will start pursuing electrical methods in situ, as laboratory measurements are at risk of over-predicting the effective diffusivity. Presently, there are research teams from Finland and the Czech Republic which perform laboratory work along these lines, with the potential outcome of performing in situ measurements in the not too distant future. However, this topic has so far gained

relatively little attention within the scientific community, and one must be humble to the fact that a larger body of researchers are required to solve some of the remaining puzzles. Accordingly, while this report provides answers to a number of questions, it also leaves some issues unanswered. Further investigations are required, as well as increased cooperation with other research teams. Fortunately, new laboratory studies are presently being planned or performed, and there is already an increase in international cooperation.

2 SSM's request for supplementary information

SSM's request for supplementary information (SSM 2013) is structured on six different items. This report intends to fully respond to item 5, and to partly respond to item 6. Responses to item 1–4, as well as to the main part of item 6, are provided elsewhere. This chapter provides the relevant paragraphs of the request concerning items 5 and 6, which are in Swedish, and translates them to English. Text from supporting documents, e.g. Haggerty (2012), that are directly referred to in the request is also provided. At the end of this chapter, a summary of SKB's interpretation of the request in item 5, and in part in item 6, is given.

2.1 The request – item 5

> *"SSM anser att SKB bör redovisa ett underlag som visar att bergets elektriska ledningsförmåga inte på ett väsentligt sätt kan störa de fältskaliga konduktivitetsmätningar som ligger till grund för parametrisering av matrisdiffusion. Förekomst av rimligt sannolika konstellationer av ogynnsamma mineralsammansättningar bör belysas (i perspektivet påverkan på konduktivitetsmätningar för att verifiera matrisdiffusion)."*

This translates to:

SSM considers that SKB should submit documentation showing that the rock's electrical conductivity cannot significantly disrupt the field-scale conductivity measurements that are the basis for the parameterisation of matrix diffusion. The occurrence of reasonably possible configurations of unfavourable mineral compositions should be highlighted (in the perspective of affecting conductivity measurements used to verify matrix diffusion).

2.2 The reasons behind the request – item 5

> *"SKB:s främsta dataunderlag för parameterisering av bergets effektiva diffusivitet baseras på mätningar av elektrisk resistivitet (se SKB 2008, sid 365) både i laboratorie- och fältskala med enbart ett fåtal direkta diffusionsmätningar. Så som påpekas av Haggerty (2012; punkt 1 appendix 2) kan dock den elektriska resistiviteten delvis vara påverkad av den aktuella mineralogiska sammansättningen av berget förutom ledningsförmågan för vattenfasen. SSM anser att SKB bör redovisa ett förtydligat underlag som visar att bergets egen elektriska ledningsförmåga inte på ett väsentligt sätt kan störa de fältskaliga konduktivitetsmätningar som ligger till grund för parametrisering av matrisdiffusion. Förekomst av rimligt sannolika konstellationer av ogynnsamma mineralsammansättningar bör belysas (ogynnsamma i perspektivet användning av elektrisk resistivitet för att verifiera matrisdiffusion)."*

This translates to:

"SKB's primary data for parameterisation of the rock's effective diffusivity are based on measurements of electrical resistivity (see SKB 2008, p 365) both in the laboratory and

field scale, with only a few direct diffusion measurements. As noted by Haggerty (2012, bullet 1, Appendix 2), however, the electrical resistivity may partly be influenced by the present mineralogical composition of the rock, in addition to the conductivity of the water phase. SSM considers that SKB should present a clarifying document, showing that the rock's own electrical conductivity cannot significantly disrupt the field-scale conductivity measurements that are the basis for the parameterisation of matrix diffusion. The occurrence of reasonably possible configurations of unfavourable mineral compositions should be highlighted (unfavourable in the perspective of using electrical resistivity to verify matrix diffusion).

In this reasoning, SSM refers to Haggerty (2012, bullet 1, Appendix 2). The corresponding text is reproduced below:

> *"1. What is the electrical conductivity of dry or unsaturated rock in situ at Forsmark, and how large is this relative to electrical resistivity of saturated rock? One of the key arguments that matrix diffusion is effectively unlimited is that the rock is electrically conductive over long distances. The assumption is that the conduction happens through water in the connected pore space. However, we need to be assured that the electrical conductivity of the rock itself is not closed to the pore-water. It would also be helpful to publish a table of the electrical conductivity of all of the minerals at Forsmark, including the trace minerals."*

2.3 The request – item 6

> *"6. SSM anser att SKB bör analysera betydelsen av rimlig sannolik variabilitet av bergets diffusivitet och dess inverkan på radionuklidtransport."*

This translates to:

SSM considers that SKB should analyse the importance of reasonably probable variability of the rock diffusivity and its impact on radionuclide transport.

2.4 The reasons behind the request – item 6

> *"Haggerty (2012; punkt 6 appendix 2) påpekar att SKB:s kvantifiering av osäkerhet och variabilitet i bergets diffusivitet sannolik är för begränsad. Haggerty baserar denna slutsats på en analys av osäkerheter hos enskilda faktorer som påverkar diffusiviteten. Denna analys antyder att det är svårt att utesluta en större variabilitet för matrisdiffusivitet i jämförelse med den som SKB förutsätter i sina beräkningar (t.ex. SKB, 2010, sid 33). SSM anser därför att SKB ytterligare bör analysera betydelsen av rimlig sannolik variabilitet av bergets diffusivitet baserad på en utökad kvantifiering/resonemang kring osäkerheter/variabilitet som påverkar diffusivitet. Denna variabilitet kan förklaras av att bergets struktur och mineralogiska sammansättning varierar längs med en strömbana."*

This translates to:

Haggerty (2012, bullet 6 Appendix 2) points out that SKB's quantification of uncertainty and variability of the rock diffusivity probably is too limited. Haggerty bases this conclusion on an analysis of uncertainties of individual factors affecting the diffusivity. This analysis indicates that it is difficult to exclude a greater variability of matrix diffusivity in comparison with what SKB assumes in its calculations (e.g. SKB

2010a, p 33). Accordingly, SSM considers that SKB should further analyse the importance of reasonably probable variability of the rock diffusivity based on an extended quantification/reasoning of uncertainty/variability affecting the diffusivity. This variability can be explained by the rock's structure and mineralogical composition that varies along a flowpath."

In this reasoning, SSM refers to Haggerty (2012, bullet 6, Appendix 2). The corresponding text is reproduced below:

"How did SKB conclude that the uncertainty in diffusivity (TR-10-52) is only 0.25 log units (multiplicative factor of 3.16), when several of the factors have uncertainties of factors of two to ten and they are multiplicative? Can you provide a justification for such a small level of uncertainty given the stated uncertainties in processes that contribute to the diffusivity?"

2.5 SKB's interpretation of the request

2.5.1 Interpretation of item 5

After having analysed the request concerning item 5, the reasoning behind the request, and the relevant sections of Haggerty (2012), SKB makes the following interpretation. It appears that SSM's major concern relates to the fact that the resistivity of the saturated rock may be influenced by the present mineralogical composition of the rock, in addition to the electrical conductivity of the water phase. Here it should be noted that the (electrical) resistivity is the reciprocal of the electrical conductivity. It is not explicitly stated by which process the minerals may influence the resistivity of the saturated rock. Accordingly, this report will discuss a broad spectrum of processes by which mineral grains may affect the saturated rock resistivity, in addition to posing geometric constraints on the microporous system. It will be shown that mineral properties affect all three main mechanisms by which electrical current may be propagated in crystalline rock, if using direct current or alternating current of relatively low frequency. These main mechanisms are:

1. Charge propagation by ionic solutes in the pore water, i.e. by so called electrolytic conduction (cf. Chapter 5).
2. Charge propagation by shifting of charges from their equilibrium position in a transient or alternating electric field, i.e. by dielectric conduction (cf. Chapter 6).
3. Charge propagation by electrons moving freely within the crystal lattices of the mineral grains, i.e. by electronic conduction[1] (cf. Chapter 2).

It will further be shown that minerals may affect the saturated rock resistivity by way of decreasing it for all of the above processes; compared to if the mineral grains would have been totally inert.

When estimating the formation factor based on electrical methods, it was early on assumed that the saturated rock resistivity ρ_r (ohm.m) is the product of the formation factor and resistivity of the pore water ρ_w (ohm.m). It was further assumed that mineral properties had such limited impact on the saturated rock resistivity that it could be

[1] Concerning the term electronic conduction, it should be noted that it is used in relation to electron propagation in solids, such as the mineral magnetite (e.g. Tsuda et al. 2000). The term does not refer to transport of electric current in electronic components.

ignored. This was under the prerequisite that the ionic strength of the pore water was high enough (e.g. Archie 1942, Skagius and Neretnieks 1986):

$$\rho_r = F_f \cdot \rho_w \qquad \text{(oversimplified equation)} \qquad \text{Equation 2}$$

As will be discussed in this report, the relation between the saturated rock resistivity and formation factor is not quite as simple, especially for dense crystalline rock, and Equation 2 can be considered as oversimplified, or even obsolete. To acknowledge this, the term apparent formation factor F_f^{app} (–) is used in the following chapters of this report:

$$\rho_r = F_f^{app} \cdot \rho_w \qquad \text{Equation 3}$$

The simplification made in Equation 2 is most likely the background to the statement in SSM's reasoning behind the request that the electrical resistivity may partly be influenced by the present mineralogical composition of the rock, in addition to the conductivity of the water phase[2]. If ignoring the fact that the impact of minerals may give rise to a significant decrease in the saturated rock resistivity, and directly using Equation 2 in combination with Equation 1, this could ultimate lead to an overestimated effective diffusivity. This would in turn be non-conservative for the safety assessment, from the perspective of radionuclide retention. Accordingly, it is a valid concern of SSM that the present mineralogical composition of the rock may disrupt the field-scale conductivity measurements that are one of SKB's bases for the parameterisation of matrix diffusion.

This present report does not only describe processes that may affect the electrical measurements from a qualitative perspective, but also aims to:

- give quantitative means of performing corrections, so that the formation factor more accurately can be estimated,
- give quantitative means of estimating the uncertainty in the estimated formation factor, where no corrections can be made.

Although Equation 2 was used when estimating the formation factor during the site investigation phase (e.g. Löfgren et al. 2006), it is important to note that raw data from the site investigations were revisited as part of SR-Site and that corrections were made (SKB 2010a, Section 6.8). Accordingly, in SR-Site a more complex relation between the saturated rock resistivity and the formation factor was assumed (cf. Chapter 5).

In Appendix 2 of Haggerty (2012), the question *"what is the electrical conductivity of dry or unsaturated rock in situ at Forsmark"* is raised. While SKB is not able to provide unsaturated conditions in situ; site specific drill core samples have been dried and their electrical conductivity has been measured, as part of responding to SSM's request. The outcome of these measurements relates to long-range (centimetre-scale) electronic conduction (cf. Chapter 4). However, as is discussed in Chapters 6 and 7, short-range electronic conduction (mm-scale or less), may be of consequence if micropores are blocked by minerals of low electrical resistivity, such as metallic minerals. The consequence for the estimated effective diffusivity, should such short-range electronic

[2] *"Så som påpekas av Haggerty (2012; punkt 1 appendix 2) kan dock den elektriska resistiviteten delvis vara påverkad av den aktuella mineralogiska samman-sättningen av berget förutom ledningsförmågan för vattenfasen."*

conduction be an issue, is discussed in a quantitative fashion based on empirical laboratory results.

As discussed in this report, and as noted in the request, properties of specific minerals may give rise to artefacts in the electrical methods, and their use for estimating the effective diffusivity. Accordingly SKB is requested to highlight the occurrence of reasonably possible configurations of unfavourable mineral compositions[3]. This is predominantly done in Chapter 4 from the perspective of long-range electronic conduction, but the issue is also discussed in Chapters 5 to 7 from the perspective of electrolytic, dielectric and short-range electronic conduction.

An almost equal concern of SSM seems to be that SKB has only performed a few direct diffusion measurements, and has primarily based the parameterisation of the rock's effective diffusivity on measurements of electrical resistivity, both in the laboratory and in the field. This concern is valid for field scale measurements, as no direct and quantitative diffusion experiment has yet been performed at the Forsmark site. Before a tunnel is built, performing such measurements is unfeasible, as reliable measurements typically are based on in-diffusion followed by overcoring. Such in situ experiments have, however, been conducted at other sites of reasonably comparable geology. Examples in Sweden are the Stripa mine and Äspö Hard Rock Laboratory, from which information has been carried to the understanding and parameterisation of matrix diffusion. Concerning laboratory measurements, the concern of SSM may be based on a misunderstanding, as SKB has performed a large number of through-diffusion experiments on site specific rock, using HTO as tracer. This report aims to bring clarity to this issue, and show how results from the through-diffusion experiments are utilized in SR-Site (cf. Chapter 3).

Finally, there are two issues that need mentioning. Firstly, when SSM and Haggerty (2012) speak in terms of the rock's own electrical conductivity[4], this has primarily been interpreted to mean the dry rock electrical conductivity, alternatively the electrical conductivity of the (dry) mineral grains that constitute the rock. Also, SSM speaks of using electrical resistivity to verify matrix diffusion[5]. SKB has not used the rock's electrical properties to verify matrix diffusion as a process, but has only attempted to verify that there exists a connected microporous network in which matrix diffusion can occur.

2.5.2 Interpretation of item 6

After having analysed the request concerning item 6, SKB makes the following interpretation. The main concern of SSM seems to be that SKB has assumed a too small range in the effective diffusivity in SR-Site, where the range includes both uncertainty and natural variability. Accordingly, SKB should provide an extended quantification/reasoning of the uncertainty/variability affecting the effective diffusivity, as well as analyse the impact of a more reasonable range in the effective diffusivity on radionuclide transport[6,7].

---

[3] "*Förekomst av rimligt sannolika konstellationer av ogynnsamma mineralsammansättningar bör belysas (i perspektivet påverkan på konduktivitetsmätningar för att verifiera matrisdiffusion).*"
[4] "*…bergets egen elektriska ledningsförmåga…*"
[5] "*…användning av elektrisk resistivitet för att verifiera matrisdiffusion…*"
[6] *"SSM anser därför att SKB ytterligare bör analysera betydelsen av rimlig sannolik variabilitet av bergets diffusivitet baserad på en utökad kvantifiering/resonemang kring osäkerheter/variabilitet som påverkar diffusivitet."*

This present report aims to respond to the part concerning uncertainty in the effective diffusivity, originating from uncertainty in the formation factor, which in turn originates from artefacts in the experimental methodologies used in the site investigations. The focus of the response is on the electrical methods, but also artefacts corresponding to diffusive methods, induced by bringing drill core samples to the de-stressed environment in the laboratory, are discussed. This ultimately leads to assigning an uncertainty range for the flowpath averaged formation factor (cf. Chapter 8), whereas in SR-Site a single point value was used (SKB 2010a, Section 6.8.10).

It should be noted that in this report, as in e.g. SKB (2010a), natural variability is excluded from the term uncertainty. The part of the request that concerns the natural variability of the effective diffusivity is discussed in another part of the response by Löfgren and Crawford[8], as is the part concerning the impact of a more reasonable range in the effective diffusivity on radionuclide transport.

[7] *SSM anser att SKB bör analysera betydelsen av rimlig sannolik variabilitet av bergets diffusivitet och dess inverkan på radionuklidtransport.*

[8] Löfgren M, Crawford J, 2014. Modelling of radionuclide retention by matrix diffusion in a layered rock model. Response to the request by SSM for supplementary information on retention of radionuclides (SSM2011-2426-110), items 4 and 6 (SKBdoc 1421960).

3 The usage of electrical methods when estimating formation factors for subsequent use in SR-Site

This chapter provides an overview of the experimental data available for SR-Site, concerning the formation factor and effective diffusivity. This overview is intentionally provided without discussing the methods by which they were obtained, and without describing artefacts and errors that may be associated with the measurements. Concerning electrical methods, such discussions are provided in the subsequent chapters of this report, where also some basic equations and theory are provided.

3.1 Experimental data available for SR-Site

In the work leading up to SR-Site, electrical methods as well as traditional through-diffusion measurements have been used to obtain formation factors and effective diffusivities. In the site investigations, it was discovered early on that formation factors obtained in situ deviate from those obtained in the laboratory. This has mainly been ascribed to the fact that the samples in the laboratory are stress released, and that a rim zone of mechanical damage exists at the sample surfaces, as result of the drilling and sawing. Figure 1 shows typical results from the Forsmark site investigation, from the borehole KFM06A at depth (Löfgren et al. 2006). The triangles mark the laboratory apparent formation factors while the purple diamonds mark the in situ apparent formation factor of the non-fractured rock matrix, as obtained by Equation 3. The purpose of displaying the figure is to indicate that the in situ and laboratory formation factors deviate by about one order of magnitude. From a safety assessment point of view, decreased formation factors lead to decreased radionuclide retention and may increase the radiological risk, and vice versa. Accordingly, the indication of lower formation factors in situ, as compared to in the laboratory, cannot be neglected.

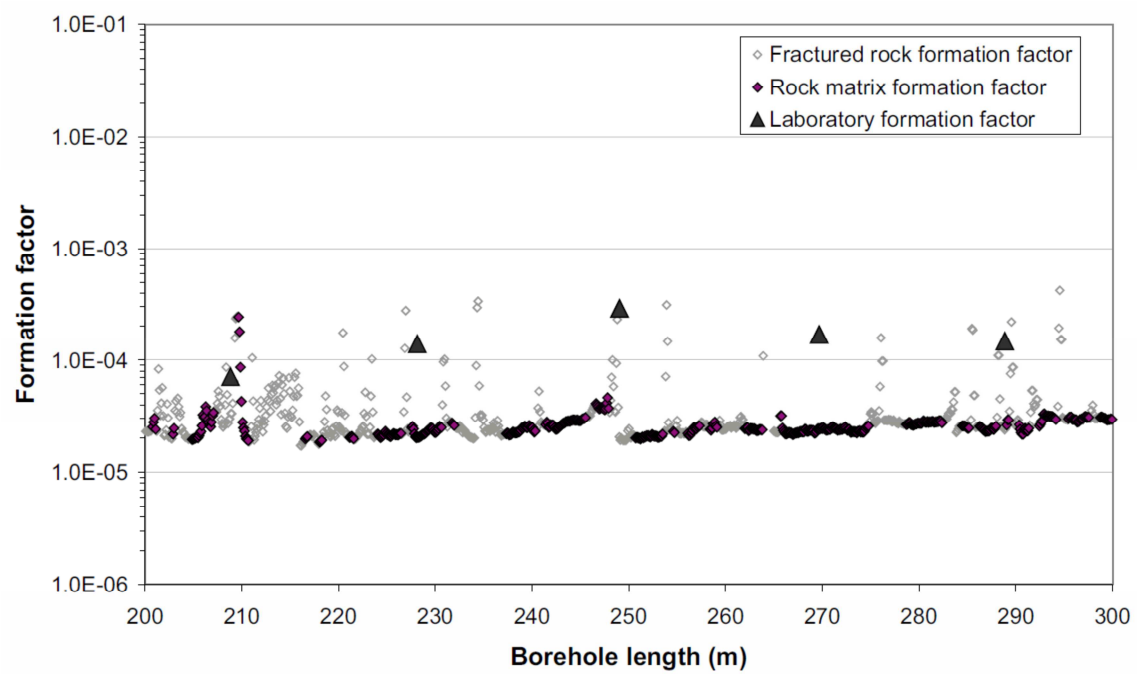

Figure 1. In situ apparent formation factors (diamonds) and laboratory apparent formation factors (triangles) obtained by electrical methods in borehole KFM06A. For what is labelled rock matrix formation factors in the figure, in situ data from drill core sections that are intersected by open fractures, detected in the drill core mapping, have been discarded. This is to assure that the electrical properties of the non-fractured rock matrix are reflected. Image reproduced from Löfgren et al. (2006, Appendix C1).

In situ formation factors have been obtained by electrical methods in numerous boreholes at the Forsmark site, as well as at the Oskarshamn site (see overview in SKB 2010b, Appendix A8). In SR-Site, it was judged that the associated data uncertainty was the lowest for boreholes KFM01D, KFM06A and KFM08C at the Forsmark site. Figure 2 shows a histogram of the over 10,000 in situ formation factor data points obtained in these boreholes.

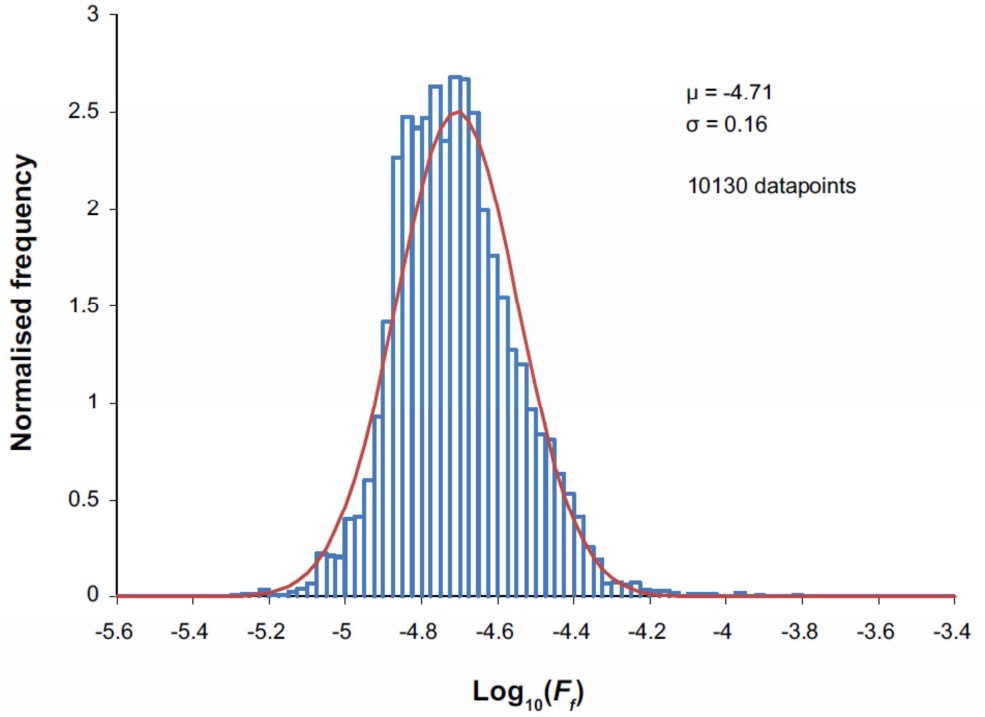

Figure 2. Histogram of all in situ formation factor data from boreholes KFM01D, KFM06A, and KFM08C, for the non-fractured rock matrix, together with the best fit log-normal distribution. Image reproduced from SKB (2010a, Figure 6-78).

This histogram can be compared to Figure 3, showing the histogram of effective diffusivity data obtained on 58 Forsmark drill core samples by laboratory through-diffusion measurements using tritiated water, HTO, as the tracer (Selnert et al. 2008). For making the comparison, the formation factor in Figure 2 needs to be converted to effective diffusivity. This is made by multiplying it with the D_w of HTO of $2 \cdot 10^{-9}$ m^2/s, which gives rise to an 8.7 log-unit shift downward in the x-axis.

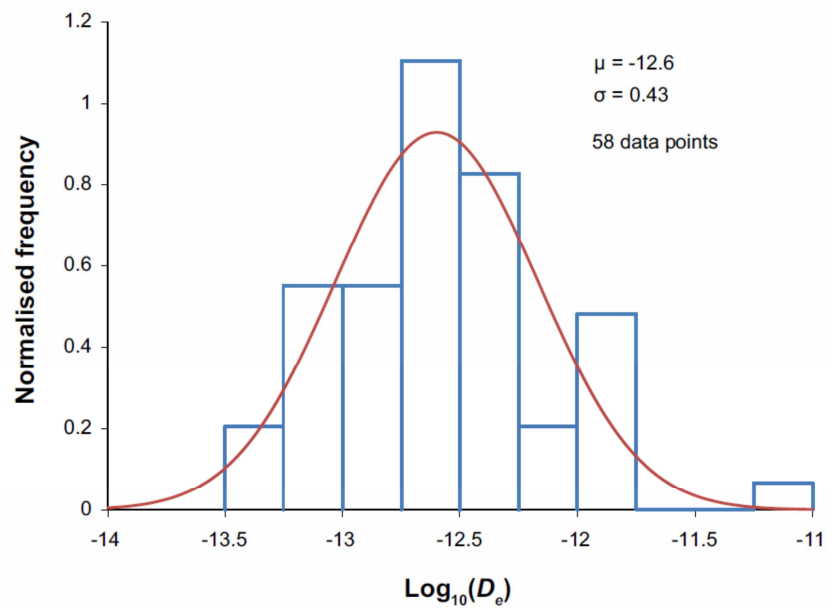

Figure 3. Histogram of all effective diffusivities from laboratory through-diffusion measurements in Forsmark, except for those of samples with porosities over 10%. Image reproduced from SKB (2010a, Figure 6-79).

In addition, to provide linkage between the in situ electrical measurements and laboratory through-diffusion measurements, the formation factor was measured by electrical methods in the laboratory. Figure 4 shows the laboratory formation factors obtained for 163 drill core samples from Forsmark, presented in the form of a cumulative distribution function (CDF). The data are shown by the red solid curve.

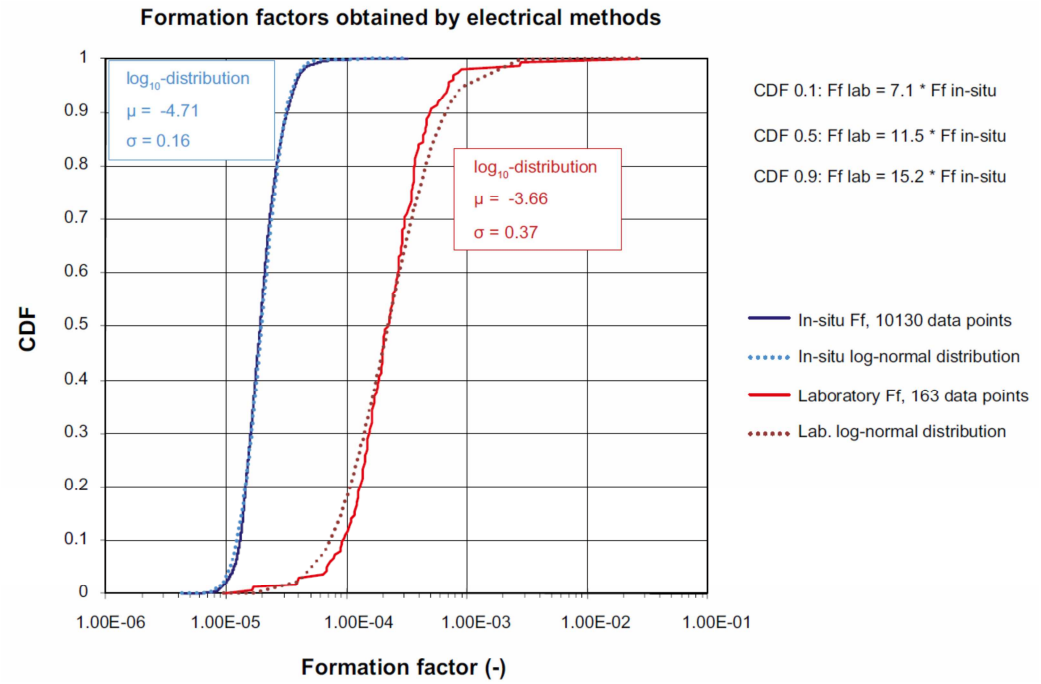

Figure 4. Blue curves: CDF and best fit log-normal distribution of in situ formation factors for borehole KFM01D, KFM06A, and KFM08C. Red curves: CDF and best fit log-normal distribution of laboratory formation factors obtained by the electrical resistivity method. Image reproduced from SKB (2010a, Figure 6-80).

3.2 Two approaches to assigning effective diffusivities in SR-Site

Based on the sets of data presented above, from the in situ electrical method, laboratory through-diffusion measurements, and the laboratory electrical method, two approaches of analysing the data were taken in SR-Site when deciding on a set of effective diffusivities for subsequent use in the safety assessment (SKB 2010a, Section 6.8).

3.2.1 First approach

In the first approach it was considered that the foremost part of data uncertainty originates in stress release and excavation induced damage, which the laboratory samples are subjected to. Accordingly, the suggested formation factor was derived based on the in situ electrical method only. This was done by taking the arithmetic mean value of all the 10,130 data points (in the normal space) of Figure 2, resulting in a best estimate, flowpath averaged, formation factor of $2.1 \cdot 10^{-5}$. By multiplying this value by a D_w of $1 \cdot 10^{-9}$ m^2/s for all cations and non-charged species, a best estimate, flowpath averaged, effective diffusivity of $2.1 \cdot 10^{-14}$ m^2/s was obtained.

The values provided in the above paragraph are said to be flowpath averaged, which deserves an explanation. For the FARF31 computational code used in the SR-Site radionuclide transport modelling (SKB 2010d), flowpath averaged values are requested as input data. This is as constant retention parameters are used for entire flowpaths in the calculations. The chosen way of providing a representative flowpath averaged value for the formation factor is to assume that each of the measured in situ formation factor data points is equally representative for the host rock. Furthermore, experimental observations point to the fact that different rock volumes at Forsmark display similar formation factors. Accordingly, pooling all representative in situ formation factors and taking their arithmetic mean provides a flowpath averaged value.

3.2.2 Second approach

In the second approach it was decided to rely on the laboratory through-diffusion measurements, as they are traditionally used throughout the scientific community when measuring the effective diffusivity of rock. However, as there are clear indications that samples in the laboratory are disturbed from either stress release or excavation induced damage, or both, there was a need to correct for this by introducing a correction factor. In early work on effects of stress release it was found that the effective diffusivity could be decreased by 20–70% percent by re-stressing the sample at high pressures (Skagius and Neretnieks 1986). However, that work was not done on rock samples from the Forsmark site, and only focused on stress release and not on excavation induced damage. Accordingly, it was decided to compare saturated rock resistivities obtained in situ and in the laboratory as a basis for estimating the correction factor.

As is discussed in the subsequent chapters, the saturated rock resistivity is not only affected by the geometric properties of the microporous system, but also by the electrical conductivity of the pore water and by a process called surface conduction. In addition, as alternating current was used in the majority of the measurements, dielectric effects may have been a disturbing factor. Finally, depending on the geology of the site, there may have been disturbance from electronic conduction. Accordingly, when comparing saturated rock resistivities measured in situ and in the laboratory, as a basis for estimating the correction factor, a number of considerations were needed. For this reason, it was judged as more transparent to first convert the in situ and laboratory

saturated rock resistivities to formation factors, making the necessary corrections, and subsequently compare the outcome.

This approach may seem strange, as there is an underlying assumption that the "true" formation factor actually can be measured by electrical methods, which is also the main assumption of the first approach. However, less emphasis is put on this underlying assumption. In this second approach the electrical methods only need to perform well enough to capture a relative change in pore space geometric properties, as result of stress release and excavation induced damage. Accordingly, by this second approach, the methods do not need to give an absolute measure of the formation factor. If the electrical methods in the laboratory and in situ are subjected to same biases, originating from, for example, electronic or dielectric conduction, these biases should cancel out. Of course, this assumption would require that the magnitude of the bias is similar for the methods applied in the laboratory and in situ, and that the bias in itself is unaffected by stress release and excavation induced damage, which is presently unknown. In spite of this unknown, it was judged that this second approach was the best available method to obtain a correction factor for stress release and excavation induced damage, short of performing in situ diffusion tests.

Two different methods have been used when comparing the in situ and laboratory formation factors obtained by electrical methods. Perhaps the most obvious way is to compare the pair of formation factors obtained at exactly the same location in the borehole; to calculate the discrepancy; and to take the average value and standard deviation of this discrepancy for a large number of paired data points. Such comparisons were made in two steps in Byegård et al. (2008, Section 3.3.3), but only for a subset of the laboratory samples. In one step, formation factors obtained by laboratory through-diffusion experiments were compared with (apparent) formation factors[9] obtained by the laboratory electrical method on the same samples. It was concluded that the electrical method provides 2.2±1.2 times higher (apparent) formation factors than the through-diffusion measurements. In the other step, through-diffusion formation factors were compared to apparent formation factors obtained by the electrical method in situ, at locations in the borehole from where the drill core samples were taken. It was concluded that the apparent formation factors obtained by the in situ electrical method were 8.3±8.9 times lower than the formation factors measured by the laboratory through-diffusion method. As can be seen, the great standard deviations make combining these sets of data uncertain, especially as the data are not necessarily normally distributed. Also, it would have been preferable if the comparisons had been made with the formation factor, and not with the apparent formation factor. One could revisit the raw data and make comparisons for the full data set of formation factors obtained by electrical methods in the laboratory (on in total 163 drill core samples) with as many corresponding in situ formation factors as possible. However, there are limitations with this approach. Firstly, in many locations the rock is too fractured to obtain the in situ formation factor representing the non-fractured rock matrix, and therefore no comparison can be made. Secondly, as the sample size in situ (m^3-scale) and in the laboratory (cm^3-scale) differs, one would not expect the paired data points to fully correspond.

A second way of analysing the data, which was adopted in SR-Site, is to present the in situ and laboratory formation factors obtained by electrical methods in the form of

[9] As the apparent formation factors have been obtained on samples saturated by a pore water of high ionic strength, the difference between the formation factor and apparent formation factor is very small.

CDFs, and then compare the shift in these CDFs. The resulting CDFs are shown above in Figure 4 where the shift, in general, is a little over one log-unit. At the 50% CDF marker, the shift is a factor of 11.5, and this number was adopted in SR-Site as the correction factor for stress release and excavation induced damage. This correction factor was applied to the 58 site specific effective diffusivities obtained in laboratory through-diffusion measurements (cf. the histogram in Figure 3), resulting in the CDF shown by the red curve in Figure 5. For comparison, the blue curve of Figure 5 represents the effective diffusivities obtained using the first approach, when only relying on the in situ data. It is based on the same data as shown in the histogram of Figure 2, but the formation factor has been multiplied by $D_w = 1 \cdot 10^{-9}$ m^2/s (cf. Equation 1).

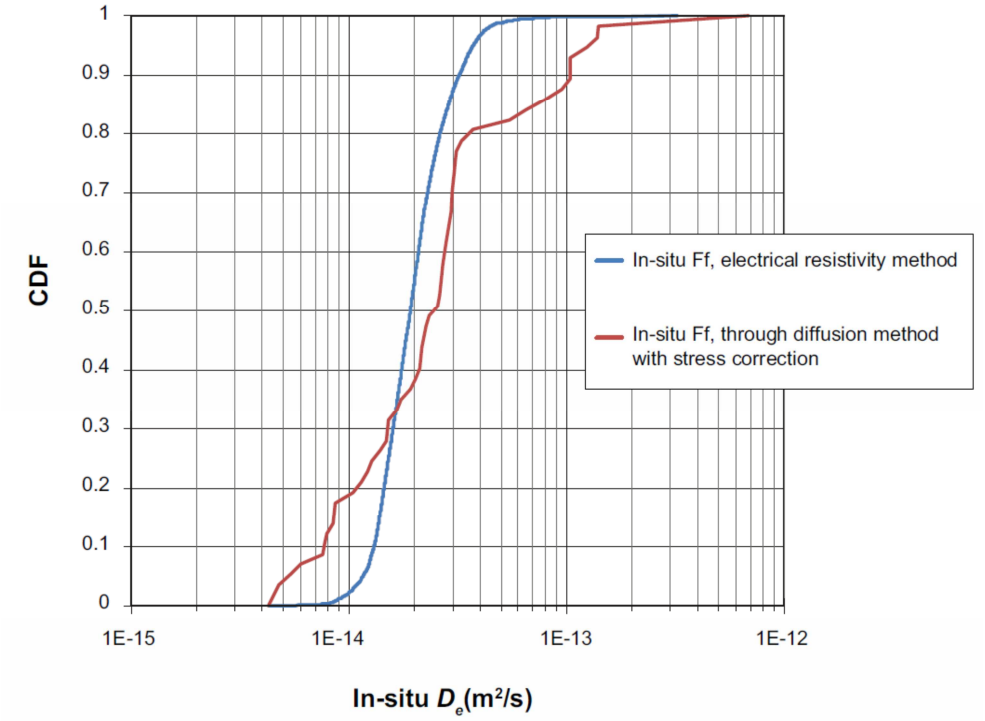

Figure 5. Comparison of CDFs of in situ effective diffusivity obtained by the two approaches of analysing data. The blue curve represents approach 1 and the red curve approach 2.

3.3 The choice of data in SR-Site

As can be seen in Figure 5, the two approaches of obtaining effective diffusivities provide similar CDFs. Moreover, by taking the arithmetic mean of each data set, both approaches give a flowpath averaged formation factor of $2.1 \cdot 10^{-5}$. Accordingly, it was decided not to favour one approach over the other. The final choice of flowpath average effective diffusivities is displayed in Table 1. In SR-Site, no uncertainty range was assigned for the flowpath averaged formation factor. Therefore, the uncertainty range in effective diffusivity in Table 1 reflects the uncertainties in D_w for the different radionuclides and groundwater constituents. For anions it was assumed that anion exclusion cause a decrease in the effective diffusivity by half a $\log_{10}$-unit (SKB 2010a, Section 6.8.7).

Table 1. Flow path averaged in situ effective diffusivity suggested for use in SR-Site. Table reproduced from SKB (2010a, Table 6-91).

Type of solute	Best estimate D_e (m^2/s)	$Log_{10}D_e$ (m^2/s) – μ	$Log_{10}D_e$ (m^2/s) – σ	Probability density function
Cations and non-charged solutes	$2.1 \cdot 10^{-14}$	–13.7	0.25	Log-normal
Anions	$6.6 \cdot 10^{-15}$	–14.2	0.25	Log-normal

In Table 1, μ and σ are the distribution parameters (mean and standard deviation) of the suggested log-normal probability density function for the effective diffusivity.

One of the aims of this chapter has been to reassure SSM that traditional through-diffusion measurements have not been neglected in the Forsmark site investigation, but that such measurements have been performed on a large number of site specific drill core samples. Furthermore, upon applying a correction factor for stress release and excavation induced damage, the resulting data have been used directly when assigning the in situ effective diffusivity for subsequent use in SR-Site radionuclide transport modelling.

4 Dry rock vs. saturated rock resistivity

4.1 Background

Electric current may be propagated in saturated rocks and minerals by electronic conduction, electrolytic conduction, and dielectric conduction (e.g. Telford et al. 1990, Section 5.2). This chapter will investigate the case where direct electric current is propagated by long-range electron movements in the crystalline mineral lattices of the Forsmark rock (electronic conduction), in addition to by migration of ionic solutes in the pore water (electrolytic conduction). In this particular chapter, the direct electric current is assumed to be either propagated in the mineral lattices or in the pore water, in parallel routes. It is assumed that there is no interaction between the two routes. Such interactions are instead discussed in Chapter 7. By this assumption, up-scaling can be done and instead of talking about the resistance of individual mineral grains, one can talk about the bulk resistance of the dry rock R_{dr} (ohm). Accordingly, the saturated rock resistance R_r (ohm) can be described by the following electrical circuit analogy, consisting of two parallel coupled resistors.

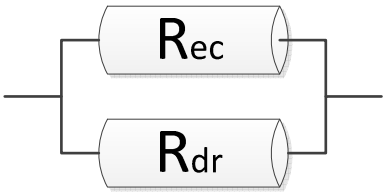

Figure 6. Parallel coupled resistors where R_{ec} represents the resistance associated with electrolytic conduction in the pore water and R_{dr} is the resistance of the dry rock.

In Figure 6, R_{ec} (ohm) represents the resistance associated with electrolytic conduction in the pore water. For a homogenous resistor of constant cross section area, such as the cylinders in Figure 6, the resistivity is the resistance times the resistor's cross section area, divided by its length. As the two resistances in Figure 6 correspond to the same rock sample, with a defined geometry, one could just as well speak in terms of the saturated rock resistivity ρ_r (ohm.m):

$$\frac{1}{\rho_r} = \frac{1}{\rho_{ec}} + \frac{1}{\rho_{dr}} \qquad \text{Equation 4}$$

Where ρ_{ec} (ohm.m) is the resistivity associated with electrolytic conduction and ρ_{dr} (ohm.m) is the dry rock resistivity.

In Forsmark, the in situ resistivity of the saturated non-fractured rock matrix is generally within the range 10,000 to 70,000 ohm.m. This can be seen in Figure 7, showing histograms of the saturated rock matrix resistivity from around the boreholes KFM01D and KFM08C (Löfgren 2007). When discussing the resistivity of minerals and dry rock in the subsequent sections, comparisons with Figure 7 can be made.

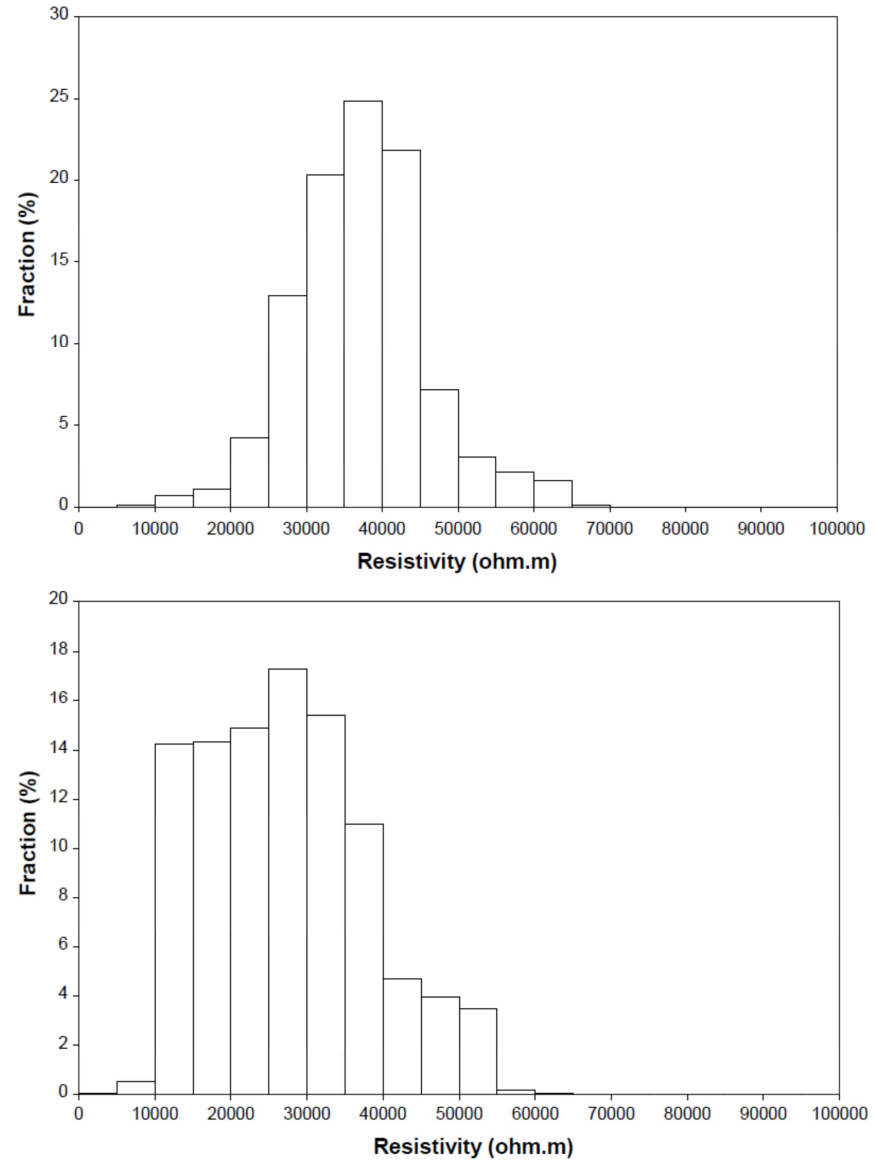

Figure 7. Upper and lower images show histograms of the saturated in situ rock matrix resistivities of KFM01D and KFM08C, respectively. Reproduced from Löfgren (2007, Figures 4-2 and 4-4).

4.2 Resistivity of the most abundant minerals in Forsmark

This section gives the mineral composition of the most common rock types in the target area at the Forsmark site, where the repository is planned to be located. This is in direct response to the request of highlighting the occurrence of reasonably possible configurations of unfavourable mineral compositions at Forsmark (cf. Section 2.1). For the most abundant minerals, their reported resistivity range is provided. These resistivity ranges come from a limited literature survey that ended up including a few standard textbooks on the matter. It has been surprisingly difficult to find the electrical resistivity of minerals at room temperature in peer-reviewed scientific articles and textbooks, where also the conditions for the measurements have been reported.

4.2.1 The abundance of minerals

Table 2 shows the volumetric proportions of different rock types in rock domains RFM029 and RFM045. These two rock domains define the rock in the target volume of Forsmark (SKB 2011, Section 4.3). For the four most abundant rock types, their mineralogical compositions are shown in Figure 8 to Figure 11. The mineralogical compositions of the remaining rock types are found in Sandström and Stephens (2009).

Table 2. Rock names and SKB codes for major and most common subordinate rock types found within rock domain RFM029 and RFM045. Approximate proportions (vol%) for each rock type is also given for both rock domains. Table reproduced from Crawford (2008, Table 4-1).

Rock name	SKB code	RFM029	RFM045
Granite to granodiorite, metamorphic, medium-grained	**101057**	73.6	18.0
Pegmatite, pegmatitic granite	**101061**	13.3	13.9
Granite, granodiorite and tonalite, metamorphic, fine- to medium-grained	**101051**	4.6	9.0
Granite, metamorphic, aplitic	**101058**	1.2	49.3
Amphibolite	**102017**	4.4	6.3
Granite, fine- to medium-grained	**111058**	1.5	1.3
Felsic to intermediate volcanic rock, metamorphic	**103076**	0.4	1.2
Calc-silicate rock (skarn)	**108019**	0.3	0.2
Quartz-dominated hydrothermal vein/segregation	**8021**	0.2	0.2
Diorite, quartz diorite and gabbro, metamorphic	**101033**	0.2	0.2

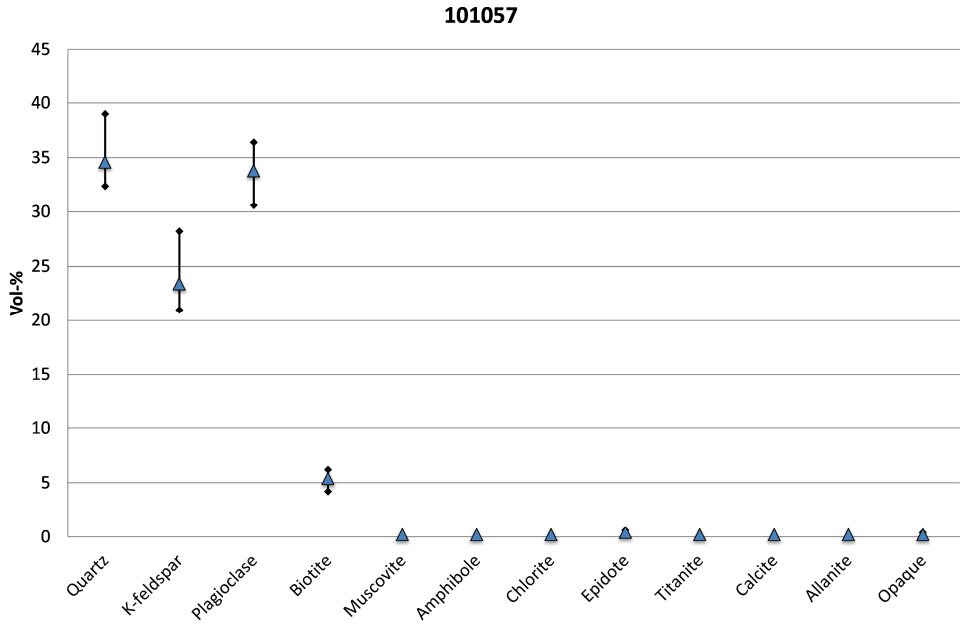

Figure 8. Mineral composition of rock type 101057 – metamorphosed, medium-grained granite to granodiorite. The whiskers show the upper and lower quartiles. Data taken from Sandström and Stephens (2009, Table 3-7).

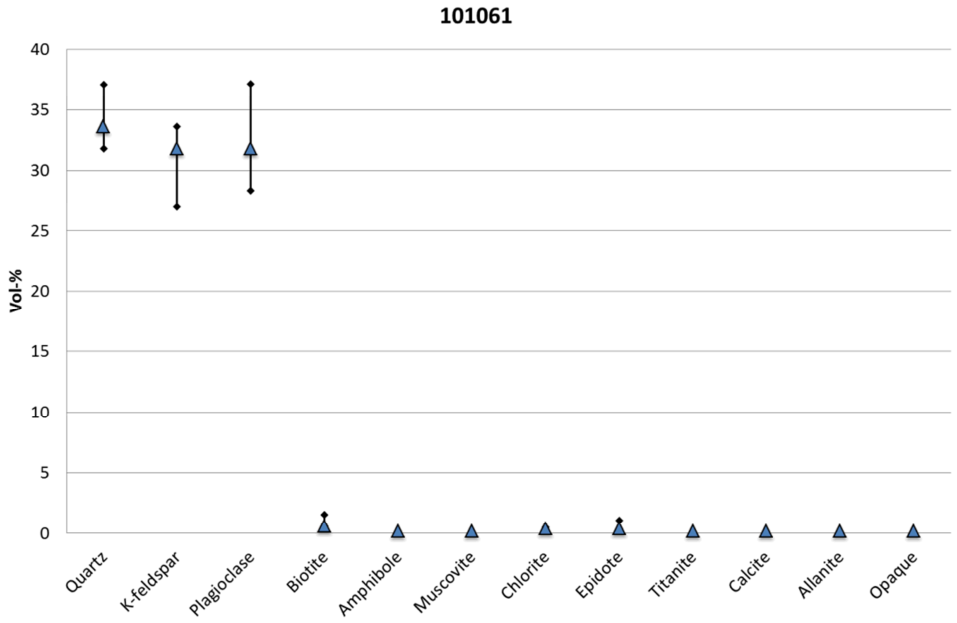

Figure 9. Mineral composition of rock type 101061 – pegmatite or pegmatitic granite. The whiskers show the upper and lower quartiles. Data taken from Sandström and Stephens (2009, Table 3-12).

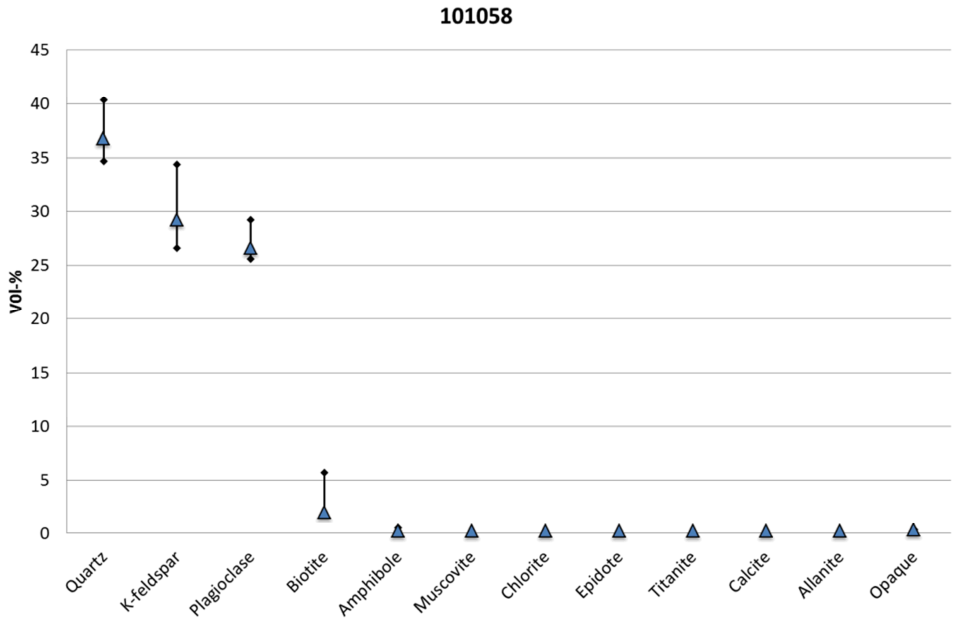

Figure 10. Mineral composition of rock type 101058 – Metamorphosed, aplitic granite. The whiskers show the upper and lower quartiles. Data taken from Sandström and Stephens (2009, Table 3-11).

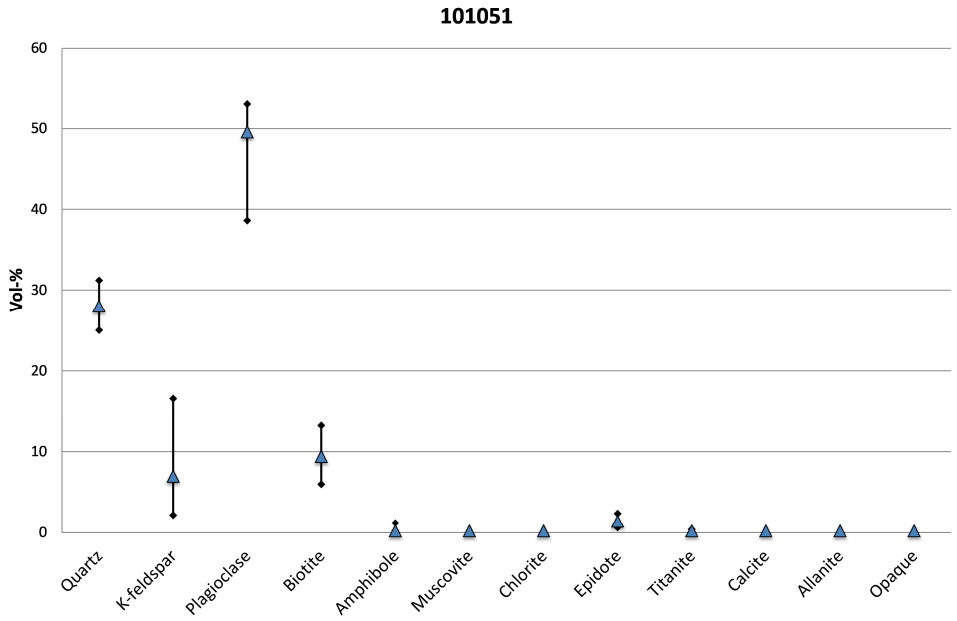

Figure 11. Mineral composition of rock type 101051 – metamorphosed, fine- to medium-grained granitoid. The whiskers show the upper and lower quartiles. Data taken from Sandström and Stephens (2009, Table 3-3).

As can be seen in Figure 8 to Figure 11, quartz, K-feldspar, and plagioclase, which are framework silicates, constitute the bulk of the rock volume at the site. Biotite, which is a sheet silicate, is in general the fourth most abundant mineral. In altered rock, biotite may have transformed to chlorite. If so, chlorite may also be of importance in terms of abundance (Sandström and Stephens 2009).

4.2.2 The resistivity of minerals

Quartz is widely known to be an electrical insulator. At room temperature, electrical resistivity values are commonly reported to be in the range of 10^{10}–10^{14} ohm.m. This is at least six orders of magnitude higher than for the saturated rock resistivity at Forsmark (cf. Figure 7). As for the other framework minerals, the (dry) resistivity decreases with increasing temperature, as often reported in the context of increased depth into the Earth's crust, and with an increasing amounts of impurities. Impurities may also give rise to an increased surface charge on the mineral grain surfaces, e.g. due to isomorphous replacement (e.g. Stumm and Morgan 1996). Such surface charge may increase both the electrolytic and dielectric conduction, should the mineral grain be surrounded by pore water in saturated rock. For various reasons there is a spread in reported resistivity data for quartz, as demonstrated in Table 3. Such a spread in resistivity can also be seen for the other minerals in Table 4 to Table 6. The data in these tables should generally represent dry mineral conditions.

Table 3. Reported electrical resistivities of quartz.

Resistivity (ohm.m)	Reference
$10^{12} – 10^{14}$	Dakhnov 1962, Table 3
$4{\cdot}10^{10} – 2{\cdot}10^{14}$	Telford et al. 1990, Table 5-1.
$10^{12} – 2{\cdot}10^{14}$	Schön 1996, Table 9.1

K-feldspar and plagioclase are groups of feldspar minerals that are electric insulators, but sometimes to a lesser degree than quartz. A few reported electrical resistivities for

K-feldspar and plagioclase are shown in Table 4. These resistivities are at least four orders of magnitude larger than for the saturated rock at Forsmark.

Table 4. Reported electrical resistivities of K-feldspar and plagioclase.

Resistivity (ohm.m)	Reference
$1.8 \cdot 10^{11}$ (microcline)	Schön 1996, Table 9.1
$1.4 \cdot 10^{12}$ (orthoclase)	Schön 1996, Table 9.1
$6.3 \cdot 10^{8}$ (labradorite)	Schön 1996, Table 9.1
$4.8 \cdot 10^{8}$ (albite)	Schön 1996, Table 9.1
10^{9} (oligoclase)	Schön 1996, Table 9.1
$7.7 \cdot 10^{9}$ (anorthite)	Schön 1996, Table 9.1

Table 5 shows a few reported resistivities of biotite. As can be seen, the reported data ranges over 13 orders of magnitude. One can suspect that the much lower values of Telford et al. (1990) were obtained in the presence of water. Due to the layered structure of biotite, the mineral surfaces are highly charged and this charge is counteracted by mobile cations in the pore water that are able to carry charge. If the suspicion of water presence is true, the data may not represent electronic conduction but may be affected by electrolytic and dielectric conduction. On the other hand, if the data do represent dry mineral resistivities, there is a chance that electronic conduction in biotite may be a factor for the dry rock resistivity. Whether or not biotite affects the dry rock resistivity must be investigated on site specific rock (as done in Section 4.3).

Table 5. Reported electrical resistivities of biotite.

Resistivity (ohm.m)	Reference
$8.3 \cdot 10^{10}$	Schön 1996, Table 9.1
$10^{14} – 10^{15}$	Dakhnov 1962, Table 3
$2 \cdot 10^{2} – 10^{6}$	Telford et al. 1990, Table 5-1

As can be seen from Figure 8 to Figure 11, the abundances of other minerals are in general very low. Accordingly, if distributed fairly evenly throughout the rock mass, they could not constitute connected routes for long-range electronic conduction. However, it is conceivable that sealed fractures could constitute connected routes into the rock matrix where electronic conduction could occur, even if the volumetric abundance of fracture minerals is low. Important fracture minerals at Forsmark are calcite, chlorite, clay minerals, pyrite, hematite, and laumontite (Byegård et al. 2008, Table 2-3, Löfgren and Sidborn 2010). The resistivity of these fracture minerals, with the exception of laumontite, is shown in Table 6. As can be seen, chlorite, clay minerals, and calcite have relatively high resistivities. On the other hand, pyrite and hematite have relatively low electrical resistivities and could affect the results, should they constitute a connected layer at the fracture surfaces. Pyrite and hematite layers were investigated in a special drill core mapping campaign at Forsmark, focusing on fracture minerals (Eklund and Mattsson 2009, Löfgren and Sidborn 2010). It was found that the two minerals occur as spots or patches on the fracture surfaces, and do not form continuous routes. No resistivity of laumontite has been found in the limited literature survey, but the zeolite structure of laumontite will provide great attraction to dissolved cations at the mineral surface, should the rock be saturated. It is reasonable to assume that this will ensure that associated electrolytic and/or dielectric conduction is much higher than

electronic conduction if the mineral grain is surrounded by pore water. Table 6 also shows the resistivity of some other minerals that may be of general interest. One example is epidote, being the fifth most abundant mineral in some important rock types at Forsmark (Sandström and Stephens 2009). Another example is magnetite, giving rise to a decreased rock resistivity at many geological sites in Sweden.

Table 6. Reported electrical resistivities of typical fracture minerals and other minerals.

Resistivity (ohm.m)	Reference
$1.6 \cdot 10^{9}$ (chlorite)	Schön 1996, Table 9.1
$10^{14} – 10^{15}$ (clay minerals)	Dakhnov 1962, Table 3
$3.7 \cdot 10^{7}$ (kaolinite)	Schön 1996, Table 9.1
$10^{11}–10^{12}$ (muscovite)	Dakhnov 1962, Table 3
$9 \cdot 10^{2} – 10^{14}$ (mica)	Telford et al. 1990, Table 5-1.
$5 \cdot 10^{12} –9 \cdot 10^{13}$ (calcite)	Schön 1996, Table 9.1
$2 \cdot 10^{12}$ (calcite)	Telford et al. 1990, Table 5-1
$10^{7} – 10^{12}$ (calcite)	Dakhnov 1962, Table 3
$10^{-4} – 10^{-1}$ (pyrite)	Schön 1996, Table 9.1
$10^{-4} – 10^{-1}$ (pyrite)	Dakhnov 1962, Table 3
$2.9 \cdot 10^{-5} – 1.5$ (pyrite)	Telford et al. 1990, Table 5-1
$1.2 \cdot 10^{-3} – 0.6$ (pyrite)	Keller and Frischknecht 1966, Table 2
$10^{-2} – 10^{6}$ (hematite)	Schön 1996, Table 9.1
$10^{4} – 10^{6}$ (hematite)	Dakhnov 1962, Table 3
$3.5 \cdot 10^{-3} – 10^{7}$ (hematite)	Telford et al. 1990, Table 5-1
$5.3 \cdot 10^{-5}$ (magnetite)	Keller and Frischknecht 1966, Table 2
$10^{-4} – 10^{-2}$ (magnetite)	Dakhnov 1962, Table 3
$5 \cdot 10^{-5} – 5.7 \cdot 10^{3}$ (magnetite)	Telford et al. 1990, Table 5-1
$4 \cdot 10^{-5}$ (magnetite)	Tsuda et al. 2000, Section 5.8
$7.7 \cdot 10^{9}$ (epidote)	Schön 1996, Table 9.1

As stated earlier, biotite may have transformed to chlorite in altered rock. Accordingly, chlorite may not only exist as fracture mineral but also as a relatively large part of the bulk rock matrix. For example, chlorite content up to 7.4 vol-% has been found in metamorphosed and oxidised, medium-grained granite to granodiorite at Forsmark (Sandström and Stephens 2009, Table 3-9). However, the impact of electronic conduction in chlorite should be insignificant, as the mineral is reported to have a relatively high resistivity (cf. Table 6).

In conclusion, it is very unlikely that long-range electronic conduction could compete with electrolytic and/or dielectric conduction in the Forsmark host rock. From this perspective, based on the above discussion, one can say that there is no configuration of unfavourable mineral compositions at Forsmark representing a large enough rock volume to generally affect the saturated rock resistivity. It is a non-controversial statement in the scientific literature that electrolytic conduction by far outweighs electronic conduction in saturated rocks that does not feature high abundances of ore (e.g. Keller and Frischknecht 1966, Section 1.4).

4.3 Measurements of dry rock resistivity of Forsmark drill core samples

In a similar fashion to the proposal by Haggerty (2012, Appendix 2, bullet 1), the dry rock resistivity has been measured on five drill core samples from the Forsmark site, as well as on four drill core samples from the Oskarshamn site. These samples have previously been used in laboratory measurements within the site investigation programme for the transport properties of rock. Previous activities include water gravimetric porosity measurements and through-diffusion (TD) tracer tests using HTO as the tracer (Selnert et al. 2008, 2009), as well as formation factor measurements by the laboratory resistivity method (Thunehed 2007a, b). In addition, these samples have been used in a special campaign aiming to investigate the relation between resistivity measurements and tracer migration experiments, in so-called through-electromigration experiments (Löfgren et al. 2009). Table 7 shows sample identification, length, rock type, as well as the formation factor F_f (–) and apparent formation factor F_f^{app} (–) reported in Selnert et al. (2008, 2009) and Thunehed (2007a, b). Table 7 is reproduced from Löfgren et al. (2009, Table 4-1), where further information on the samples can be found.

Table 7. Description of samples. Table is reproduced from Löfgren et al. (2009, Table 4-1).

Sample	Site	Borehole	Borehole length (m)	Rock type code[1]	Sample length (mm)[2]	F_f^{app} electrical methods	F_f HTO through-diffusion[3]
1	Forsmark	KFM01A	312.66 – 312.67	101057	10.25	$2.06 \cdot 10^{-4}$	$1.41 \cdot 10^{-4}$
2	Forsmark	KFM01A	312.54 – 312.55	101057	10.18	$1.66 \cdot 10^{-4}$	$9.39 \cdot 10^{-5}$
3	Forsmark	KFM02A	554.60 – 554.61	101051	12.64	$1.85 \cdot 10^{-4}$	$1.78 \cdot 10^{-4}$
4	Forsmark	KFM02A	554.71 – 554.72	101051	11.66	$1.89 \cdot 10^{-4}$	$1.50 \cdot 10^{-4}$
5	Forsmark	KFM02A	554.84 – 554.85	101051	11.38	$1.85 \cdot 10^{-4}$	$1.41 \cdot 10^{-4}$
6	Oskarshamn	KLX04	489.49 – 489.50	501036	9.68	$8.05 \cdot 10^{-5}$	$6.13 \cdot 10^{-5}$
7	Oskarshamn	KLX04	489.61 – 489.62	501036	9.85	$3.50 \cdot 10^{-5}$	$2.63 \cdot 10^{-5}$
8	Oskarshamn	KSH02	474.47 – 474.48	501030	10.29	$2.21 \cdot 10^{-5}$	$2.39 \cdot 10^{-5}$
9	Oskarshamn	KSH02	474.66 – 474.67	501030	10.27	$4.45 \cdot 10^{-5}$	$4.46 \cdot 10^{-5}$

[1] Rock codes: 101051: Granite, granodiorite and tonalite, metamorphic, fine- to medium-grained. 101057: Granite to granodiorite, metamorphic, medium-grained. 501030: Fine-grained dioritoid (metavolcanite, volcanite). 501036: Quartz monzonite to monzodiorite, equigranular to weakly porphyritic.

[2] Measured in this study by Vernier calliper.

[3] Calculated from effective diffusivities in /Selnert et al. 2008, 2009/ using the $D_w = 2.13 \cdot 10^{-9}$ m²/s for HTO.

New measurements were carried out in late 2013 at the research institute ÚJV a.s. in Řež, Czech Republic, by the same team performing the experimental work reported in Löfgren et al. (2009). The dry rock resistivity was measured by the setup illustrated in Figure 12.

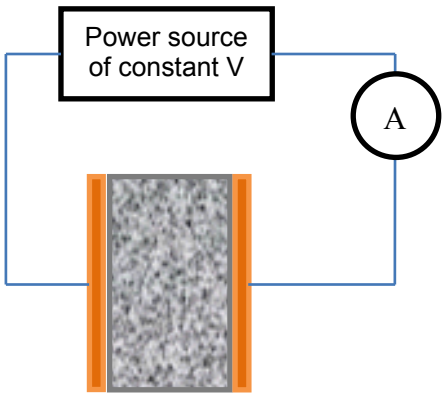

Figure 12. The dry rock resistivity of the cylindrical drill core sample is measured by directly pressing copper electrodes to its end surfaces, connected to an AC/DC power supply providing constant potential drop, and an Ampere-meter.

Prior to the measurements, the samples were dried for 48 hours at 105 °C, ensuring low enough levels of residual moisture to not affect the dry rock resistivity. Resistivity measurements were made by placing copper plates (electrodes) directly to the cross section areas of the drill core sample. The rock surfaces were judged to be smooth enough to provide good contact between rock and electrodes. No solution or gel was applied between the electrodes and rock surfaces, as electronic conduction was to be investigated. The current running through the sample was measured as applying a known and constant potential drop over the sample. The rock resistivity was calculated by using Ohm's law. In doing this, the sample was assumed to be homogenous.

When dealing with dry rock samples, their resistance becomes so high that special equipment is needed for the measurements. In a first experimental run, the equipment at hand at the department performing the measurements was used. By this equipment, the sample resistivity was measured to be at least $5{\cdot}10^{7}$ ohm.m when using a direct current (DC) power source and at least $5{\cdot}10^{5}$ ohm.m when using an alternating current (AC) power source at the frequencies 10, 100, and 2,000 Hz. It was soon discovered that these values do not reflect the actual rock resistivity, but the different measurement limits of the used Ampere-meter[10]. As a result, new measurements were performed at another department within the institute, using a DC power source of higher voltage (500 V) and an Ampere-meter able to measure the resulting current on the order of 10^{-10} A. The resulting rock resistivities, now in the range $6.9{\cdot}10^{10}$ to $4.8{\cdot}10^{11}$ ohm.m, are shown in Table 8. No AC measurement could be performed with the more sensitive equipment. Accordingly, the AC values in Table 8 are set as $>5{\cdot}10^{5}$ ohm.m, as measured by the first set of equipment.

Table 8. Dry rock resistivities as measured by direct current and alternating current.

Forsmark	**Sample 1**	**Sample 2**	**Sample 3**	**Sample 4**	**Sample 5**
DC (ohm.m)	$3.8{\cdot}10^{11}$	$1.4{\cdot}10^{11}$	$4.8{\cdot}10^{11}$	$3.4{\cdot}10^{11}$	$3.6{\cdot}10^{11}$
AC 10–2,000 Hz (ohm.m)	$>5{\cdot}10^{5}$	$>5{\cdot}10^{5}$	$>5{\cdot}10^{5}$	$>5{\cdot}10^{5}$	$>5{\cdot}10^{5}$
Oskarshamn	**Sample 6**	**Sample 7**	**Sample 8**	**Sample 9**	
DC (ohm.m)	$5.0{\cdot}10^{10}$	$3.4{\cdot}10^{10}$	$2.4{\cdot}10^{10}$	$6.9{\cdot}10^{10}$	
AC 10–2,000 Hz (ohm.m)	$>5{\cdot}10^{5}$	$>5{\cdot}10^{5}$	$>5{\cdot}10^{5}$	$>5{\cdot}10^{5}$	

[10] The measurement limit was different for AC and DC.

These results should be compared with resistivities of the same samples, as saturated by solutions of similar electrical conductivity (EC) and salinity as in situ at the sites. Such measurements have been made in Löfgren et al. (2009) using 0.05 M or 0.1 M NaCl solutions for saturating the samples, which well represents the Forsmark and Oskarshamn in situ conditions at depth. In Table 9, the saturation solution and its electrical conductivity, as well as the saturated rock resistivities measured at different frequencies, are shown. In Löfgren et al. (2009) the measurements were reproduced two or three times, and the values shown in Table 9 are the average values of the different runs.

Table 9. Saturated rock resistivities at different frequencies and pore water compositions. Resistivity data are averaged based on raw data in Löfgren et al. (2009, Appendices A and B), as reproduced in Appendix A.

Forsmark	Sample 1	Sample 2	Sample 3	Sample 4	Sample 5
Pore water composition[1]	0.1 M NaCl	0.1 M NaCl	0.05 M NaCl	0.1 M NaCl	0.05 M NaCl
EC[2] of pore water (S/m)	1.20	1.13	0.59	1.06	0.57
DC (ohm.m)	2,377	6,207	4,515	2,415	4,367
AC 10 Hz (ohm.m)	1,649	5,314	3,825	2,300	3,809
AC 100 Hz (ohm.m)	1,618	5,180	3,769	2,298	3,712
AC 2000 Hz			3,613		
Oskarshamn	**Sample 6**	**Sample 7**	**Sample 8**	**Sample 9**	
Pore water composition	0.1 M NaCl	0.05 M NaCl	0.1 M NaCl	0.05 M NaCl	
EC of pore water (S/m)	1.12	0.58	1.11	0.60	
DC (ohm.m)	1,351	3,114	3,944	3,484	
AC 10 Hz (ohm.m)	1,111	2,775	3,421	2,951	
AC 100 Hz (ohm.m)	1,105	2,653	3,344	2,911	
AC 2000 Hz (ohm.m)				2,943	

[1]The pore water composition refers to the bulk part of the pore, and not the electric double layer (cf. Chapter 5).
[2]EC (electrical conductivity) is the reciprocal to electrical resistivity and is measured in Siemens per metre.

4.4 Consequence for formation factor estimations in SR-Site

By comparing the results in Table 8 with those in Table 9 it can be seen that the dry rock resistivities are many orders of magnitude larger than the saturated rock resistivities, at all frequencies. Therefore, centimetre-scale electronic conduction in the mineral lattices, i.e. from one side of the sample to the other, is of insignificant importance. This is in agreement with the assumptions of SR-Site, based on the mineralogy of the Forsmark rock, standard textbook descriptions (cf. Section 4.2), and previous experience (e.g. Löfgren 2004).

Relating to item 6 of SSM's request, concerning the uncertainty in the flowpath averaged formation factor, there will be no added uncertainty in response to the recently performed measurements of the dry rock resistivity.

5 Electrolytic conduction and the effect of surface conduction

5.1 Background

As evident from the previous chapter, electric current propagation by electrolytic and/or dielectric conduction dwarfs that of long-range electronic conduction in the saturated rock at the Forsmark site. If applying a direct electrical field over the rock, electrolytic conduction would also dwarf dielectric conduction, especially at steady state conditions. By electrolytic conduction, ionic solutes are free to move over distances beyond those which would only induce polarization. In other words, the ionic solutes are free to move in the same porous system, and over the same distances, as diffusing solutes in the rock matrix. Accordingly, electromigration in crystalline rock, as associated with electrolytic conduction, may very well be a good analogy to matrix diffusion. This would, if so, be an extension of the analogy between electromigration and diffusion in unconstrained solution, as described by the Einstein relation.

In the very early work of formation factor determination by electrical methods, in sedimentary rock, it was proposed that the saturated rock resistivity was a product of the formation factor and the resistivity of the saturation fluid (cf. Equation 2), where the saturation fluid was a brine (Archie 1942). Here, the formation factor can be described as a purely geometric factor, signifying the geometric constraints that the porous system puts on the migrating ionic solutes associated with the electrolytic conduction. Three important things should be noted about the observations by Archie (1942).

- Firstly, the solution that saturated the rock was a brine. Accordingly, it was of very low electrical resistivity and high ionic strength.
- Secondly, sedimentary rock was discussed, being much more porous than the common rock types at Forsmark. This and the above issue guarantee a plenitude of ionic solutes available for electrolytic conduction in the bulk part of the pore water.
- Thirdly, according to the terminology used in Archie (1942), the formation factor is the saturated rock resistivity divided by the pore water resistivity, providing a number larger than one. However, by the terminology used by SKB, as well as within the field of radioactive waste management for decades (e.g. Neretnieks 1980), the (apparent) formation factor corresponds to the pore water resistivity divided by the saturated rock resistivity, providing a number smaller than one.

Although Archie (1942) predicted a linear relation between the saturated rock resistivity and the pore water resistivity, this was soon shown to be erroneous for many situations (e.g. Waxman and Smits 1968). In low-porous crystalline rock, there is a significant non-linearity between the saturated rock resistivity and the bulk pore water resistivity (e.g. Löfgren et al. 2009), which can be explained as follows. Electrolytic conduction in saturated rock is not only due to migration of ionic solutes in the bulk part of the pore water. Due to specifics of the atomic lattices of most mineral grains, their surfaces are always negatively charged (in natural groundwaters). This negative charge must be counteracted by a surplus of cations attracted towards the surface, in order to maintain

electro-neutrality. The surplus of cations are conceptualised to occupy the so-called electrical double layer, and part of these cations are dissolved and mobile (e.g. Stumm and Morgan 1996). As these cations are mobile, they are available for electrolytic conduction. In this report, as well as within the scientific community (e.g. Revil and Glover 1997), the term surface conduction is used for electrolytic conduction by the surplus of cations in the electrical double layer. As these cations are required to maintain electro-neutrality, they cannot be leached out even if the rock sample is equilibrated with distilled water. Depending on the surface charge and surface area of the mineral, the number of mobile cations available for surface conduction will differ. Accordingly, this is a case where the resistivity of the saturated rock may partly be influenced by the present mineralogical composition of the rock, in addition to the conductivity of the water phase, as identified in SSM's reasoning behind the request – item 5[11] (cf. Section 2.2).

The non-linearity between the saturated rock and pore water resistivities was identified decades ago for sedimentary rock (e.g. Waxman and Smits 1968) and was attributed the clay content of the rock. The electrostatic forces between clay minerals (generally sheet silicates) and ionic solutes are much larger than between quartz and feldspars (framework silicates) and solutes. This can, for example, be seen from the increased cation exchange capacity of clays, relative to framework silicates (e.g. Crawford 2010, Section 2.1). Therefore, the contribution from surface conduction is expected to be much larger in clays (e.g. van Olphen and Waxman1956). In the rock types of interest at Forsmark, the non-linearity has a somewhat different mineralogical explanation, as the clay content is generally low (except for in some rock immediately bordering fractures). As can be seen from Section 4.2.1, the most abundant minerals at Forsmark are quartz, K-feldspar and plagioclase, while the sheet silicate biotite comes in fourth place. Based on these mineral abundances, it can be suspected that biotite takes on special importance for the surface conduction. However, it is also conceivable that electrostatic interactions between framework mineral surfaces and ionic solutes are of significance in the Forsmark host rock, although the matter has not been a focus of attention in investigations performed by SKB.

The electrical resistance associated with electrolytic conduction can be described by an electrical circuit analogy consisting of two parallel coupled resistors, as illustrated in Figure 13a. In the figure, R_w (ohm) is the resistance associated with ionic solutes in the bulk of the pore water and R_s (ohm) is the resistance associated with surface conduction. By using the electrical circuit analogy of Figure 13, it is assumed that the two routes for conduction are independent, which is further discussed below.

[11] *"Så som påpekas av Haggerty (2012; punkt 1 appendix 2) kan dock den elektriska resistiviteten delvis vara påverkad av den aktuella mineralogiska sammansättningen av berget förutom ledningsförmågan för vattenfasen."*

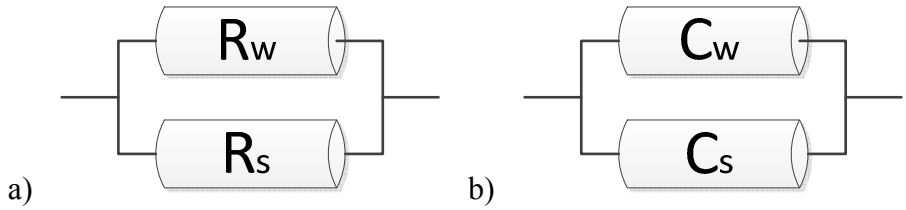

Figure 13. a) Parallel coupled resistors where R_w (ohm) represents the resistance associated with electrolytic conduction in the bulk part of the pore water and R_s (ohm) represents the resistance associated with surface conduction. b) Parallel coupled conductors where C_w (S) is the conductance associated with electrolytic conduction in the bulk part of the pore water and C_s (S) is the conductance associated with surface conduction.

As this chapter focuses on electrolytic conduction, it is appropriate to also describe the electrical circuit analogy in terms of two conductors coupled in parallel, as shown in Figure 13b. Here, the upper and lower conductances C_w (S) and C_s (S) correspond to electrolytic conduction in the bulk of the pore water and surface conduction, respectively. In fact, a theoretical discussion in terms of conduction becomes more straightforward when explaining the non-linearity between the saturated rock and pore water resistivities. If, in analogy to Ohm's law, multiplying the surface conductance by the length L (m) of the rock sample, and dividing the product by the sample cross section area A (m^2), one would get the surface conductivity κ_s (S/m):

$$C_s = \frac{A}{L} \cdot \kappa_s \qquad \text{Equation 5}$$

Concerning the pore water in the bulk of the pore, outside of the electrical double layer, its intrinsic electrical conductivity κ_w (S/m) should depend on its composition. If the rock sample is equilibrated with a surrounding electrolyte, the electrical conductivity of the bulk pore water is often assumed to equal that of the surrounding electrolyte. It can be further assumed that the thickness of the electrical double layer is very small compared to the typical micropore aperture, even though this assumption may be challenged for the smallest pores. Under these assumptions, the formation factor F_f describes the geometric constraints on electrolytic conduction by solutes in the bulk pore water, compared to electrolytic conduction in the unconstrained surrounding electrolyte. The electrolytic conduction in the bulk of the pore water can thus be described by:

$$C_w = \frac{A}{L} \cdot F_f \cdot \kappa_w \qquad \text{Equation 6}$$

The electrical conductance through the rock sample C_r (S) can be calculated by adding C_s and C_w, under the assumption that electronic and dielectric conduction can be neglected. If written in terms of conductivities, the saturated rock electrical conductivity κ_r (S/m) becomes:

$$\kappa_r = F_f \cdot \kappa_w + \kappa_s \qquad \text{Equation 7}$$

The assumption that the surface conductivity is independent of the bulk pore water ionic strength is based on the notion that the number of cations available for surface

conduction is determined by the negative charge of the mineral grains. However, according to the electric double layer theory, the thickness of the double layer is affected by the ionic strength of the bulk pore water. This could affect the ionic mobility of the cations in the electric double layer (van Olphen and Waxman 1956, Olin et al. 1997). If such an effect was pronounced, a deviation from linearity, as predicted by Equation 7, would be seen if plotting the electrical conductivity of the saturated rock versus that of the bulk pore water. Such a check is described in the below section.

5.2 Experimental work on the importance of surface conduction

As has been discussed in a number of recent SKB reports (e.g. SKB 2010a, Löfgren et al. 2009, Crawford 2008, Crawford and Sidborn 2009), experimental data substantiate the notion of significant surface conduction. This is indicated by a non-linearity between the saturated rock resistivity and pore water resistivity. This was, for example, demonstrated in Löfgren et al. (2009) on Sample 1 from the Forsmark site (cf. Table 7), which was saturated by a number or NaCl solutions of different concentrations. In Löfgren et al. (2009), resistivity measurements were reproduced two or three times, and the values shown in Table 10 are the average values of the different runs.

Table 10. Saturated rock resistivities of Sample 1 at different frequencies and pore water compositions. Data are averaged based on raw data in Löfgren et al. (2009, Appendix A).

	0.001 M NaCl	0.03 M NaCl	0.05 M NaCl	0.1 M NaCl	1.0 M NaCl
Pore water EC (S/m)	0.017	0.38	0.61	1.20	8.68
Pore water resistivity (ohm.m)	59.2	2.62	1.63	0.84	0.12
DC (ohm.m)	29,281	6,690	4,171	2,377	353
AC 10 Hz (ohm.m)	10,118	4,937	3,464	1,649	267
AC 100 Hz (ohm.m)	9,178	4,965	3,351	1,618	267

This chapter will only focus on the direct current (DC) data in Table 10, as they represent the electrolytic conduction and should be undisturbed by dielectric conduction. The alternating current data of Table 10 are further discussed in Chapter 6. In Figure 14 (left), the DC rock resistivities are plotted versus the (bulk) pore water resistivities of Table 10, clearly showing the non-linearity. In Figure 14 (right) the same data are shown, but as converted to electrical conductivities. In addition, a linear fitting is made to the data, according to Equation 7.

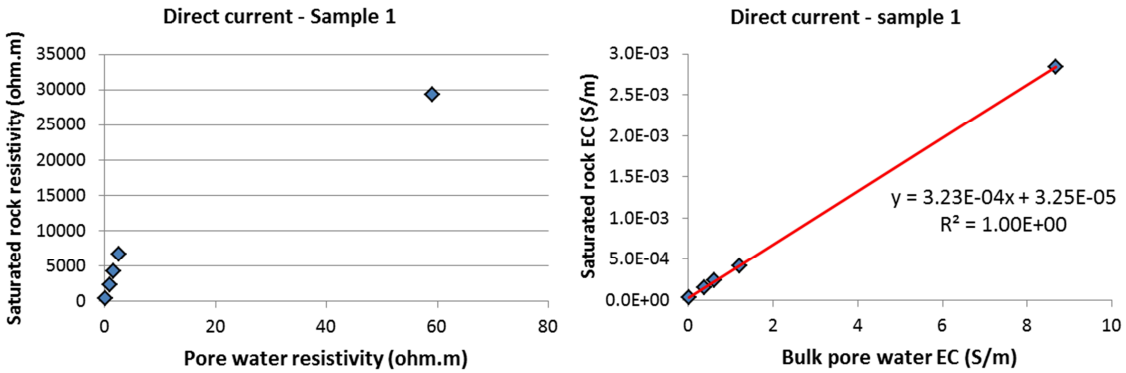

Figure 14. Left: DC saturated rock resistivity plotted vs. the pore water resistivity of Table 10. Right: DC saturated rock conductivity vs. pore water EC of Table 10. Red curve represents a linear fitting according to Equation 7, where the fitting parameters are shown. The data are obtained on a drill core sample from Forsmark (cf. Table 7).

As can be seen in Figure 14 (right), there is no pronounced deviation from linearity, providing support to the usage of Equation 7. From the slope and intercept of the linear fitting, a formation factor of Sample 1 of $3.23 \cdot 10^{-4}$ and surface conductivity of $3.25 \cdot 10^{-5}$ S/m can be deduced. The assumption of linearity, leading up to Equation 7, is currently being further investigated within the Finnish Repro project (overview in Aalto et al. 2009), and the results are monitored by SKB.

In earlier experiments made to investigate the magnitude of the surface conductivity, a great number of rock samples from the Oskarshamn site investigation area were saturated by, and equilibrated with, a solution of very low ionic strength (deionized water). Upon equilibration, the electrical conductivity of each sample was measured by using alternating current at a frequency of around 100 Hz. By ignoring possible dielectric effects, the measured electrical conductivity was assumed to correspond to the surface conductivity (Ohlsson 2000, Löfgren 2001). By re-saturating and re-equilibrating the same samples with a 1 M NaCl solution, of a high and known electrical conductivity, the rock electrical conductivity was re-measured and the apparent formation factor could be calculated by using Equation 2. It should be noted that at such high ionic strength pore water, the deviation between the apparent formation factor and the formation factor can be neglected. In spite of this, the apparent formation factors of Ohlsson (2000) and Löfgren (2001) have been recalculated to formation factors, by iteration (cf. Equation 9), and are shown by diamonds and squares in Figure 15, together with the surface conductivities. The linear relation shown in Figure 15 is based on these two data sets. In addition, in Figure 15, a triangle marks the results from Sample 1 from Forsmark (Löfgren et al. 2009, Section 6.7). This data point was obtained in a similar manner as the others (saturation and equilibration with both high and low ionic strength solutions) but the conductivity measurements were made by using direct current. Accordingly, it is safe to say that this data point is undisturbed by dielectric conduction.

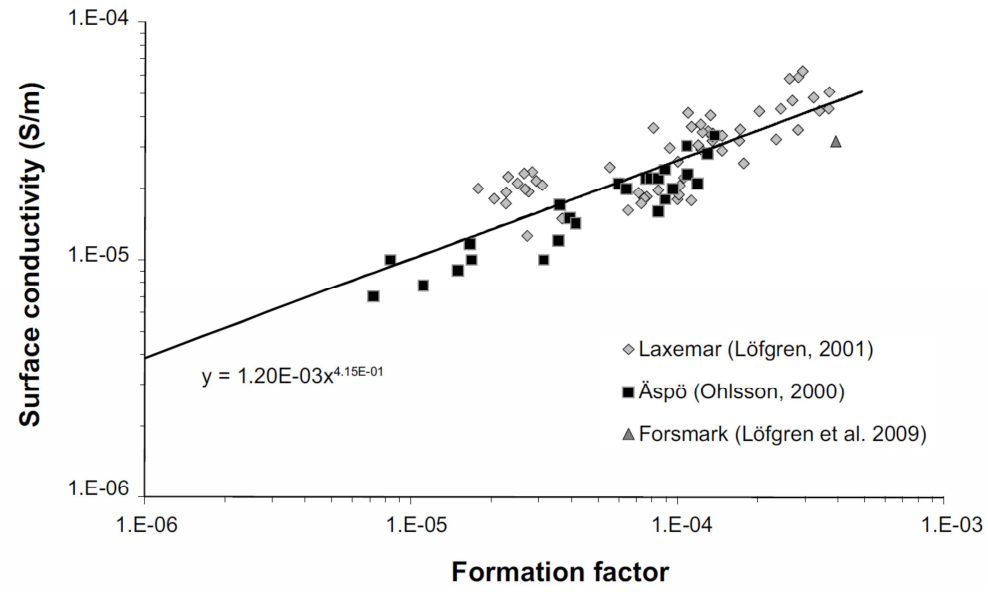

Figure 15. Surface conductivity vs. formation factor. Based on measurements on crystalline rock samples from the Oskarshamn and Forsmark sites. Reproduced from SKB (2010a, Figure 6‑72).

For unknown reasons, Figure 15 indicates a positive correlation between the surface conductivity and the formation factor:

$$\kappa_s = 0.0012 \cdot {F_f}^{0.415}$$ Equation 8

Since the completion of SR-Site, the same positive correlation has been seen for Finnish rock, within the Repro project (unpublished data). In addition, if using reinterpreted experimental data from relevant rock types from North America, found in Brace et al. (1965) and Brace and Orange (1968), they line up around the correlation, as shown in Figure 16. An additional change to Figure 16, compared to Figure 15, is that the data point from Forsmark (the triangle) has been reinterpreted. The new values are based on the slope (formation factor) and intercept (surface conductivity) of Figure 14.

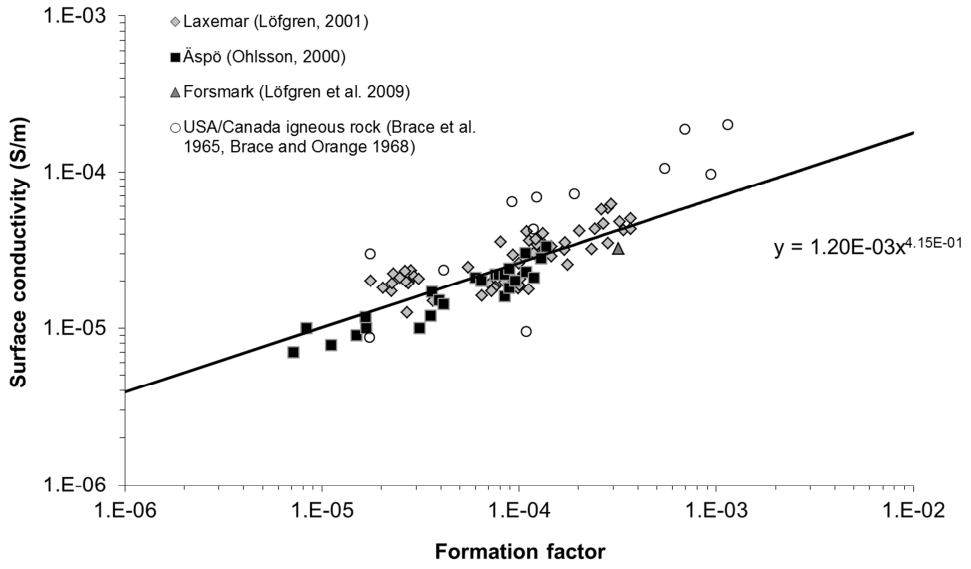

Figure 16. Surface conductivity vs. formation factor. Data from Ohlsson (2000) and Löfgren (2001), as well as the correlation, are the same as in Figure 15. Added data points come from reinterpretations of experimental data in Brace et al. (1965) and Brace and Orange (1968). Data point from Forsmark is reinterpreted, based on Figure 14.

5.3 Handling in SR-Site

In the work on radionuclide retention properties leading up to SR-Site, is has been assumed that electrolytic conduction in the bulk pore water is a valid analogue for matrix diffusion. However, there is some concern that surface conduction would be a poor analogue for matrix diffusion. For some cations such as strontium, which sorb chiefly by ion exchange, surface diffusion has been suggested to give an increased migration rate (e.g. Ohlsson and Neretnieks 1998), but this mechanism does not appear to operate for all cations. Furthermore, surface conduction would not represent the matrix diffusion of anions. Accordingly, the decision was made in SR-Site to try to negate the surface conduction contribution when estimating the formation factor by electrical methods. This was done by assuming that the surface conductivity is independent of the (bulk) pore water composition, as long as one stays within the range of naturally occurring groundwater compositions at the site. This requires, for example, that there is no pronounced change in pH and no significant exchange of monovalent cations for divalent cations in the pore water, or vice versa. If abiding to these prerequisites, and accepting the positive correlation between the surface conductivity and formation factor shown in Figure 15, the electrical conductivity of the saturated rock can be described by combining Equation 7 and Equation 8:

$$\kappa_r = F_f \cdot \kappa_w + 0.0012 \cdot {F_f}^{0.415} \qquad \text{Equation 9}$$

This equation was used in SR-Site when estimating the formation factor from electrical methods, as evident from (SKB (2010a, Equation 6-29). As seen in Equation 9 it only includes the saturated rock conductivity and (bulk) pore water electrical conductivity, except for the formation factor. Therefore, by revisiting raw data from the site

investigations in terms of saturated rock resistivities and pore water electrical conductivities, the formation factor can be estimated.

5.4 Consequence for formation factor estimations in SR-Site

As stated previously, it was assumed that the formation factor equals the apparent formation factor during the site investigations (e.g. Löfgren et al. 2006). To give an indication of the importance of accounting for surface conduction when estimating the formation factor from electrical methods, some simplistic calculations and illustrations are provided below. This is done by calculating the saturated rock resistivity as a function of pore water resistivity, by using either Equation 9 or Equation 2 (i.e. neglecting surface conduction). This is done for two different formation factors, where the first is the flowpath averaged in situ formation factor recommended for SR-Site (i.e. $2.1 \cdot 10^{-5}$). The second is the median value of the 58 formation factors obtained by laboratory through-diffusion experiments and shown in Figure 4, i.e. $1.3 \cdot 10^{-4}$. The resulting saturated rock resistivities are shown in Figure 17, for the pore water resistivity range 0.01–100 ohm.m.

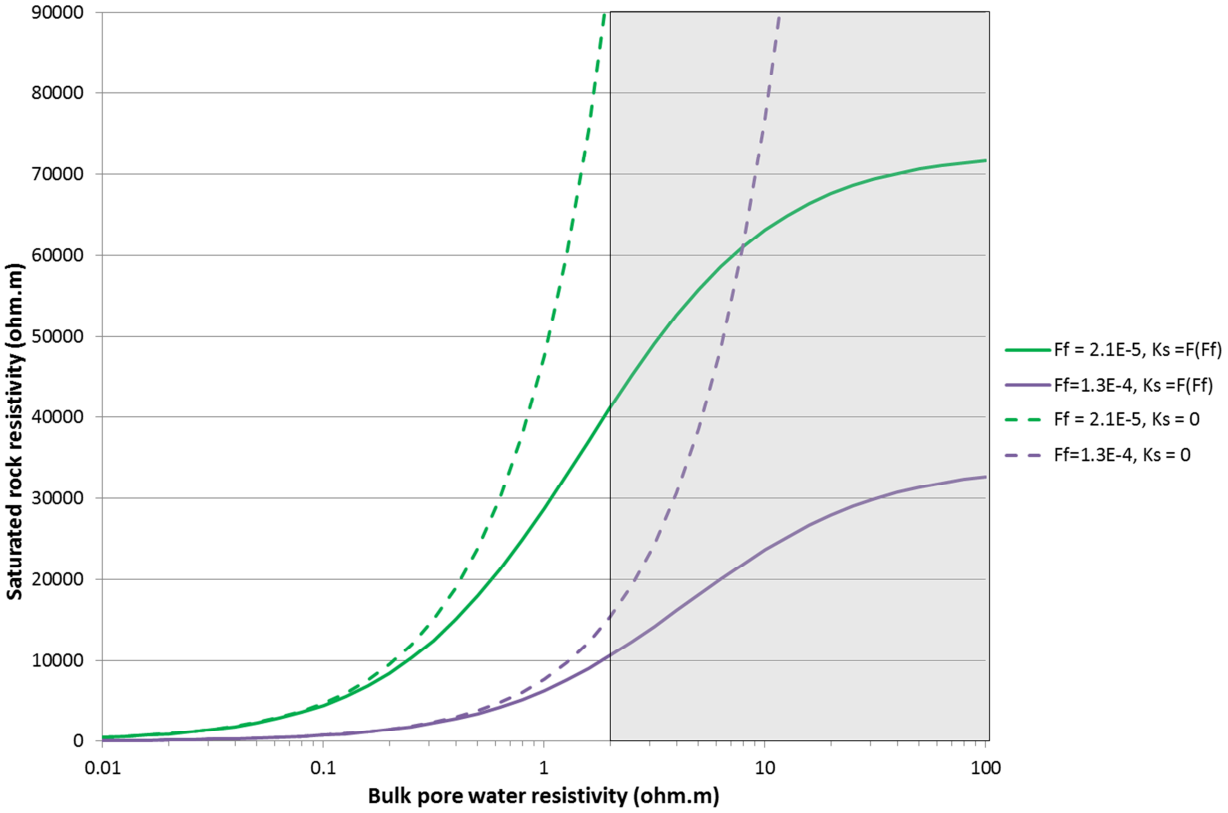

Figure 17. Saturated rock resistivity vs. bulk pore water resistivity. The solid lines correspond to calculations by Equation 9, where the surface conduction is a function of the formation factor. The dashed lines correspond to calculations by Equation 2, neglecting surface conduction. The shaded area shows pore water resistivities from which no formation factor has been derived in SR-Site.

As can be seen from Figure 17, surface conduction becomes significant for the in situ rock resistivity at pore water resistivities well below 1 ohm.m, as indicated by the point where the green dashed and solid curves deviate. For stress-released and possibly excavation damaged laboratory samples, surface conduction becomes detectable at pore water resistivities above ~1 ohm.m. For the in situ formation factor $2.1 \cdot 10^{-5}$, surface conduction outweighs the electrolytic conduction in the bulk of the pore water if the

pore water resistivity is larger than 1.5 ohm.m. At the Forsmark site, the groundwater/pore water resistivity is generally close to 1 ohm.m at repository depth, as measured on numerous occasions by the Posiva difference flow meter (e.g. Väisäsvaara et al. 2006, Appendix 11), within the hydrogeochemical site investigation program (e.g. Nilsson et al. 2006), as well as by drill core sample leaching (e.g. Waber and Smellie 2005). This indicates that, at repository depth, the majority of the electrolytic conduction occurs by solutes in the bulk of the pore water, which is the process that is intended to be studied. In shallower rock at Forsmark, however, the groundwater resistivity may be considerably higher than 1.5 ohm.m. To avoid too much uncertainty induced by surface conduction when obtaining in situ formation factors by electrical methods, a site investigation methodology was applied requesting that all data should be discarded from borehole sections having a groundwater/pore water resistivity higher than 2 ohm.m (at the in situ temperature). To highlight this precaution, the area above the pore water resistivity 2 ohm.m is shaded in Figure 17.

From the modelled results above, it becomes apparent that surface conduction plays an important role for the in situ saturated rock resistivity, and consequently for the formation factor estimations. For this reason it is somewhat unsatisfying that there only exist one data point from the Forsmark site linking the surface conductivity and the formation factor. For this reason, it is difficult to discuss the occurrence of reasonably possible configurations of unfavourable mineral compositions, as requested by SSM. What can be generally said is that the Forsmark rock, and also the Oskarshamn rock, has limited clay content. Concerning biotite, which is a mineral suspected to play an important role for the surface conduction at Forsmark, its abundance is similar at the Forsmark and Oskarshamn sites (Sandström and Stephens 2009, Drake et al. 2006). The fact that data from different sites, also from North America, line up around the correlation in Figure 16 is reassuring. It indicates that minor site specific deviations in mineralogy are of little consequence the surface conductivity contribution. An estimate of how much the scatter in Figure 15, as well as other uncertainties associated with in situ electrical measurements, affects the estimated formation factors is provided in Crawford (2012), together with the conclusion that impact is relatively limited.

It should be noted that most of the data in Figure 15 and Figure 16 are obtained by using alternating current. Accordingly they are to some extent affected by dielectric conduction, which manifests in overestimated surface conductivities and formation factors. As is further discussed in Chapter 6, dielectric effects become more pronounced the higher the pore water resistivity is. If so, the surface conductivities of Figure 15 and Figure 16 should be overestimated to a higher degree than the formation factors. This would result in an over-correction for the surface conductivity when using Equation 9, which would result in underestimated formation factors. This would be agreeable from the perspective of the safety assessment and radionuclide retention, as it would be conservative. In Section 6.1, a single data point indicates that the surface conductivity may be overestimated by a factor of about two, when measured by alternating current.

Part of item 6 of SSM's request concerns the uncertainty in the flowpath averaged formation factor recommended for SR-Site, i.e. $2.1 \cdot 10^{-5}$. In the following, this single point value is used in a few simplistic calculations. The aim is to see what the corresponding recalculated formation factor would be if assuming that the surface conductivity, for this particular formation factor, was overestimated by a factor of two when using Equation 8. The originally assumed surface conductivity can be calculated to be $1.4 \cdot 10^{-5}$ S/m. If assuming a pore water resistivity of 1 ohm.m, the apparent formation factor can be calculated to be $3.5 \cdot 10^{-5}$. If reducing the surface conductivity to

$0.7 \cdot 10^{-5}$ S/m, and recalculating the formation factor from the apparent formation factor, the result would be $2.8 \cdot 10^{-5}$, which is relatively close to the original formation factor.

It is recognised that there is a gap in knowledge on the surface conductivity as measured by direct current for different formation factors. The above paragraph illustrates the magnitude of the error that may be induced in the formation factor estimates when using Equation 9. With present day knowledge, it is not possible to make a more elaborate recalculation of the formation factor, but one must accept that there is an element of uncertainty originating in the used correlation between the formation factor and surface conductivity, as measured by alternating current. Based on present day knowledge it is judged that the uncertainty should be constrained within a factor less than two. To conclude, the surface conduction has been reasonably well corrected for in SR-Site. The remaining uncertainty should be small enough not to impact the results from the radionuclide transport calculations to a significant degree.

6 Dielectric conduction and its consequences for formation factor estimations

6.1 Properties of the micropore system evoking dielectric effects

A dielectric material is an electrical insulator that can be polarized by an applied electric field. When placed in an electric field, its electric charges do not flow through the material as they do through a conductor, but only slightly shift from their average equilibrium positions. This causes dielectric polarization. When discussing measurements of the dielectric behaviour of rock, this is often done in terms of induced polarization. A good starting point when catching up on these matters is Telford et al. (1990, Chapter 9).

In circuit theory, a capacitor would be a dielectric. Direct current cannot run through the capacitor, except for during the swift charge and discharge periods when turning the potential gradient on and off. However, if applying an alternating potential gradient over the capacitor, especially at high frequency, alternating current can seemingly be propagated through it. Crystalline rock has features on the microscale that remind of capacitors, mainly as the mineral grains are electrically charged and as their surfaces feature an electrical double layer (cf. Section 5.1). The mineral surfaces, and their impact on the electrical field in the pore water, is illustrated in Figure 18 showing four different features of the microporosity that may bring about dielectric behaviour. It should be imagined that the alternating potential field is horizontal in the figure, where the red arrows indicate the areas where dielectric effects occur.

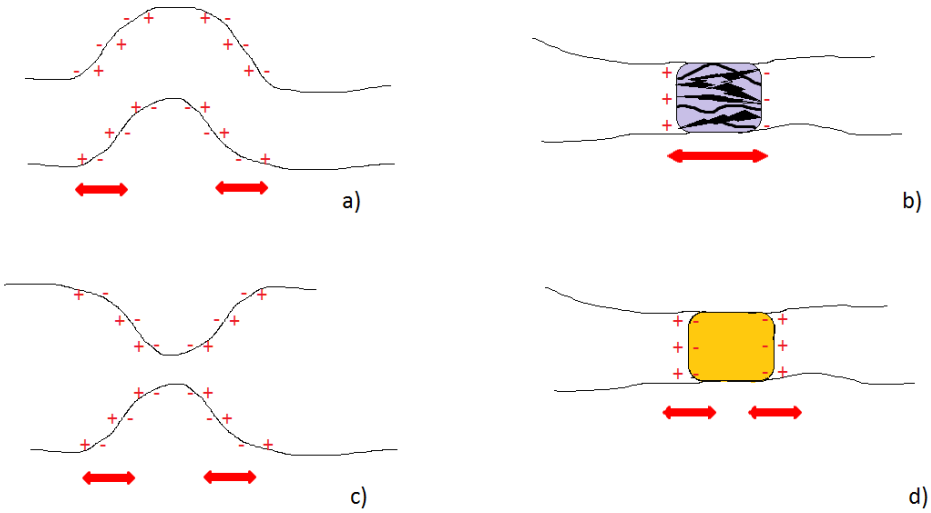

Figure 18. Illustrations of microscale features of the rock's porous system that may cause dielectric behaviour. The red arrows indicate zones of capacitance effects.

Figure 18 a) and c) show pores that are tortuous and constrictive, respectively, bounded by negatively charged mineral surfaces. In the illustrations, the bounding minerals can be assumed to be quartz or feldspars, i.e. electrical insulators having negatively charged surfaces. This negative charge is counteracted by more or less mobile cations in the

electric double layer. Parts of the mineral surfaces are at an angle to the alternating field. Accordingly, associated charges can be shifted in their relative position as response to the electric field and thus display a dielectric behaviour.

Figure 18 b) illustrates a pore that is occupied by porous clay minerals; a case that has been observed in crystalline rock (e.g. Siitari-Kauppi et al. 2010). Due to the highly charged clay surfaces, and its narrow pores, there is severe anion exclusion. When applying a potential gradient over the clay particle, the anion concentration at one side of the particle will build up, while it will be depleted on the other side. This reminds of ion selective membranes, and the process is often referred to as membrane polarization (e.g. Telford et al. 1990, Section 9.2.2). It is frequently said to be the most prominent polarization mechanism in the average rock that is poor in ores. Two things should be noted on membrane polarization. Although it is frequently assigned to the clay content of rock, other sheet silicates such as biotite may exhibit similar behaviour, although the effect may be reduced. It should be further noted that membrane polarization also can occur in the constricted pore of Figure 18 c), if the pore aperture is small enough in respect to the thickness of the electric double layer; allowing for anion exclusion effects. The degree of membrane polarization is of special interest when estimating the matrix diffusivity of anions through electrical methods. If the degree of membrane polarization is high, it could mean a severe anion exclusion effect that would lower the effective diffusivity of anions. However, if not care is taken, such anion exclusion could remain undetected in an alternating electric field, as the current may be propagated through the rock, by dielectric effects, without being significantly impacted.

Figure 18 d) shows another case of special interest when estimating the matrix diffusivity of rock through electrical methods. Here a metallic mineral grain blocks the pore. Alternatively one can say that the metallic mineral grain short circuits two nearby micropores. It should be noted that the metallic minerals of interest are not in their pure or native metal form, but can be used to produce metals. Examples of metallic minerals are magnetite, which is an oxide, and pyrite, which is a sulphide. As their abundance of metallic elements is high, in many cases their electrical resistivity is low (cf. Table 6). These minerals generally display negatively charged mineral surfaces. As such they may display dielectric behaviour (cf. Telford et al. 1990, Section 9.2.3), even if metallic minerals are not electrical insulators and therefore strictly are not dielectrics. In addition, electrochemical reactions may occur at the different sides of the mineral grain providing a link between electrolytic conduction and electronic conduction. Accordingly, also direct current may run through the blocked pore. In this case, ionic reactants are transported to one side of the blocking mineral grain by electrolytic conduction, reaction occurs at the mineral surface, free electrons are conducted in the metallic mineral grain, reaction again occurs at the other side of the mineral grain, and ionic reaction products are transported away by electrolytic conduction. However, it should be noted that for each reaction there is a loss in energy, which manifests in reaction resistances and resembles ohmic dissipation[12]. Accordingly, if using a direct current this would give rise to an unexpectedly high resistivity. It is somewhat troublesome to note that when estimating the effective diffusivity by such methods, this could be interpreted as a lower effective diffusivity in an otherwise connected microporous system, when in fact the microporous system may be non-connected. If using alternating current, the added reaction resistance could easily be masked by the dielectric behaviour of the system, and therefore remain undetected. The potential blocking of micropores is further discussed in Chapter 7.

[12] Loss of electric energy when a current flows through a resistance due to conversion into heat.

6.2 Describing dielectric effects by circuit theory

In attempts to explain the electrical behaviour or rock, the rock has been simplified to electric circuits mimicking its potential/current response (e.g. Telford et al. 1990, Section 9.2.4). For the cases where no reaction occurs, but where there are capacitance effects, e.g. in the electric double layer, the circuit in Figure 19 can be applied.

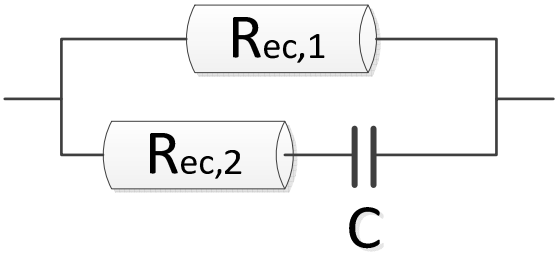

Figure 19. Electric circuit representation of rock, including capacitance effects in the electric double layer.

In Figure 19 the upper route that is purely resistive and represents electrolytic conduction, both in the bulk part of the pores and in the electrical double layer parallel to the electric field. Accordingly, $R_{ec,1}$ (ohm) is the resistance associated with the entire electrical circuit analogy of Figure 13. In the lower route, the capacitor C represents the dielectric conduction, for example in the electric double layer oriented normal to the potential gradient, working as a capacitor. However, electrolytic conduction needs to lead up to these mineral surfaces. Accordingly, a resistor $R_{ec,2}$ (ohm) that is similar to resistor $R_{ec,1}$ is inserted in the circuit. In cases where there is not only capacitance effects in the electric double layer, but also reactions at metallic minerals, membrane polarization, etc. the capacitor in Figure 19 is exchanged for an element of frequency dependent resistance, generally referred to as impedance Z (ohm) (cf. Telford et al. 1990, Figure 9.3), as shown in Figure 20. This impedance then includes all processes in parts of the pores where current conduction is frequency dependent. Alternatively, the two routes in Figure 20 represent two parallel pores, one featuring resistance effects only while the other also features impedance effects.

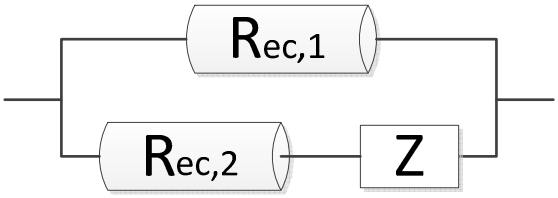

Figure 20. Electric circuit representation of rock, including frequency dependent impedance effects in the pores. Adapted from Telford et al. (1990, Figure 9.3).

When measuring the electrical resistance of rock described by the circuit of Figure 19, using direct current, it will correspond to that of $R_{ec,1}$ as soon as the charging of the capacitor C is complete and no current can take the lower route. However, when using and alternating electric field, current can take the lower route by (partial) charging and discharging of the capacitor, resulting in a impedance of the circuit that is lower than that of $R_{ec,1.}$ Here the impedance is defined as the amplitude in voltage over the circuit divided by the amplitude in current running through the circuit. As the impedance is frequency dependent, it is complex and has a real and imaginary part. The real part is the resistance R while the imaginary part is the reactance X (ohm). As such, $Z = R + iX$,

where *i* is the imaginary unit. In Figure 21, the relations between resistance, impedance and reactance is shown in a phasor, as linked through the phase angle.

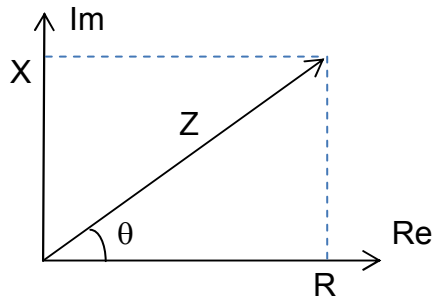

Figure 21. The relations between impedance Z, resistance R, reactance X, and phase angle θ.

The angle between the complex impedance and its real part, the resistance, is called the phase angle θ (° or rad). If the phase angle is 0°, there is no capacitance effect and the impedance equals the resistivity. If the phase angle is 90°, there are only capacitance effects.

6.3 Errors originating in dielectric effects

In the above section it has been shown that the true resistance of a rock sample may be underestimated if measured by alternating current, if assuming the resistance to be equal to the impedance, and if the induced polarisation is significant. If one, for example, accepts that the impedance and resistance deviates by up to 1% without evoking a need for corrections, the maximum phase angle would be 8°. Figure 22 shows the phase angle of 39 drill core samples from Forsmark and 59 drill core samples from Oskarshamn, measured with alternating current at the frequency 0.1 Hz (Thunehed 2007a, c, d). All samples were saturated by a 1 M NaCl solution, i.e. a solution of higher ionic strength than expected in situ. As can be seen, most phase angles are below 1°, with an average of 0.17° for the Forsmark samples. A phase angle of 0.17° would mean a deviation between the impedance of resistance of about 0.001%. Accordingly, capacitance effects in Forsmark rock can be neglected when measuring at such low frequencies, under the applied conditions.

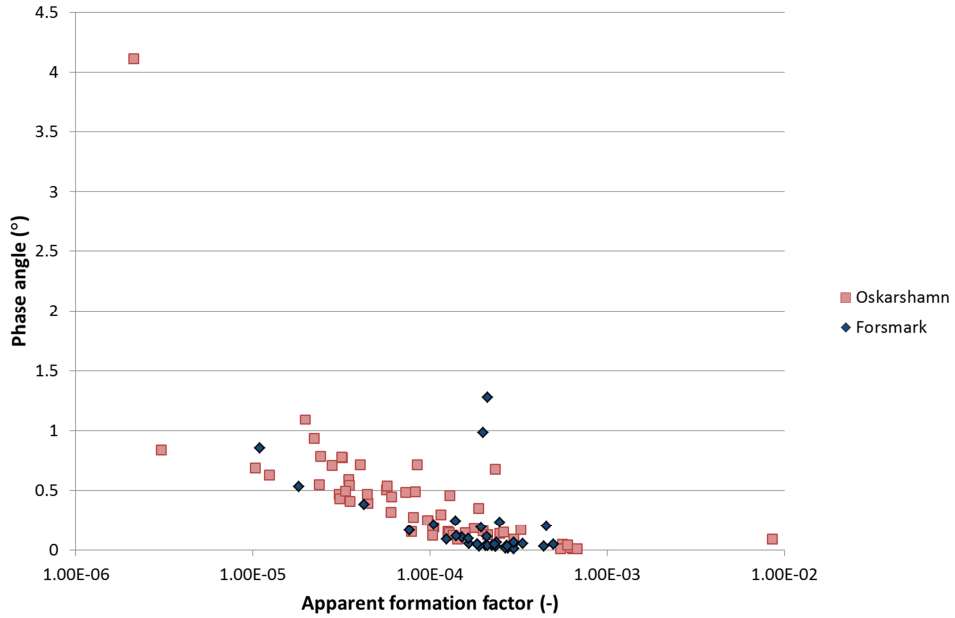

Figure 22. Phase angles for Forsmark and Oskarshamn rock samples saturated by 1.0 M NaCl, at 0.1 Hz. Based on tabulated data appended in Thunehed (2007a, c, d).

It should be noted, however, that the result in Figure 22 cannot be taken as a guarantee that dielectric effects can be neglected in all rock resistivity measurements at Forsmark. Firstly, the frequency used, 0.1 Hz, is very low compared to the 2,000 Hz used in rock resistivity measurements in situ. Secondly, as a pore water solution of high ionic strength is used, electrolytic conduction in the bulk of the pore water is expected to dominate. This would not necessarily be the case at the low ionic strength pore waters existing in shallow rock at the Forsmark site. Thirdly, the measurements are performed on stress released samples in the laboratory. As one can see from Figure 22 the phase angle increases slightly with decreasing apparent formation factor[13]. However, the effect seems to be minor and Figure 22 suggests that phase angles on the order of 1° can be expected for formation factors equal to those in situ. A phase angle of 1° would only induce a deviation between the impedance and resistance of about 0.02 %.

Figure 23 shows how the phase angle varies with frequencies up to 30 Hz for one Forsmark sample judged as anomalous, and one Forsmark sample judged as normal and representative for the site (Thunehed 2007b). As can be seen, the phase angle of the normal sample increases with increasing frequency. For the anomalous sample, the phase angle peaks at 2 Hz and decreases thereafter. In spite of this, the saturated rock resistivity decreases with increasing frequencies in the entire frequency range. Such behaviour cannot be described by the simplified discussion above. On the other hand, such anomalous samples have proved to be rare at the Forsmark site.

[13] As the apparent formation factors have been obtained on samples saturated by a pore water of high ionic strength, the difference between the formation factor and apparent formation factor is very small.

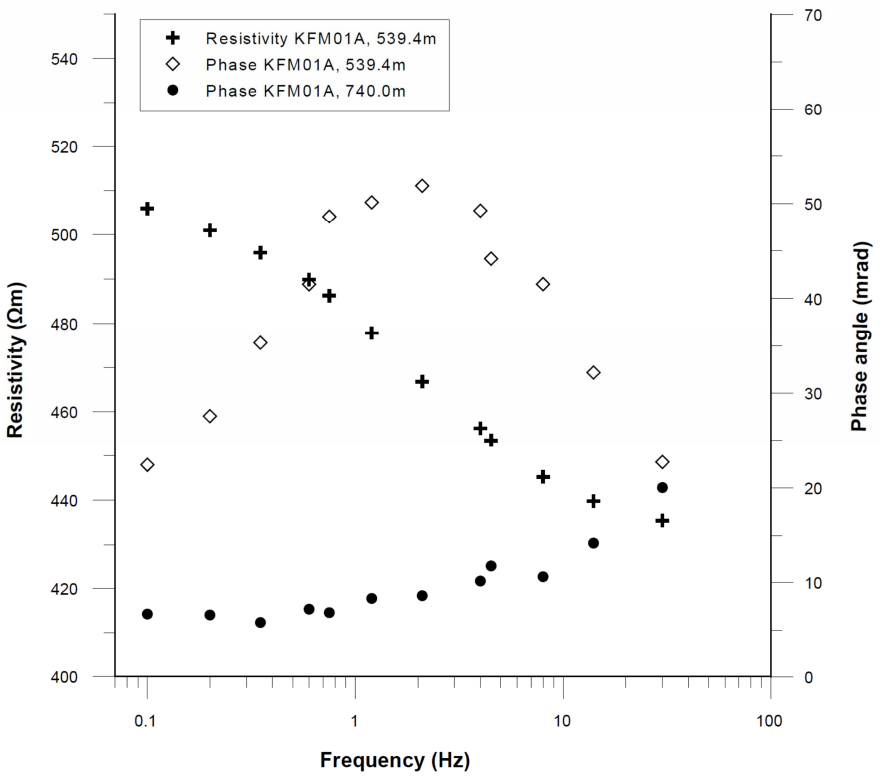

Figure 23. Resistivity (ohm.m) and phase angle (mrad) plotted versus measurement frequency for an anomalous sample (KFM01A, 539.39–539.42 m). Phase angle results for a normal sample (KFM01A, 740.01–740.04 m) are shown for reference. Figure reproduced from Thunehed (2007b, Figure 5-3).

No phase angle has been measured for frequencies above 30 Hz for Forsmark rock. However, impedance spectroscopy has been done for two samples from the Oskarshamn site (Löfgren 2001); one saturated by 1 M NaCl and the other by deionised water. Figure 24 and Figure 25 show how the impedance varies with frequency in the range 0.05 to 500.000 Hz.

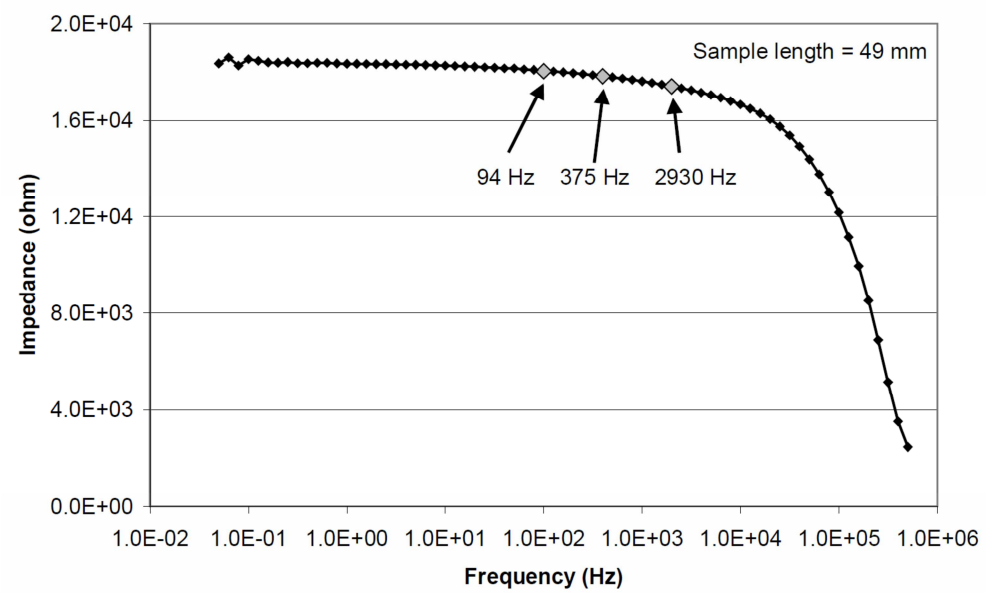

Figure 24. Impedance spectroscopy of Laxemar sample saturated with 1 M NaCl. Reproduced from Löfgren (2001, Figure 5-15).

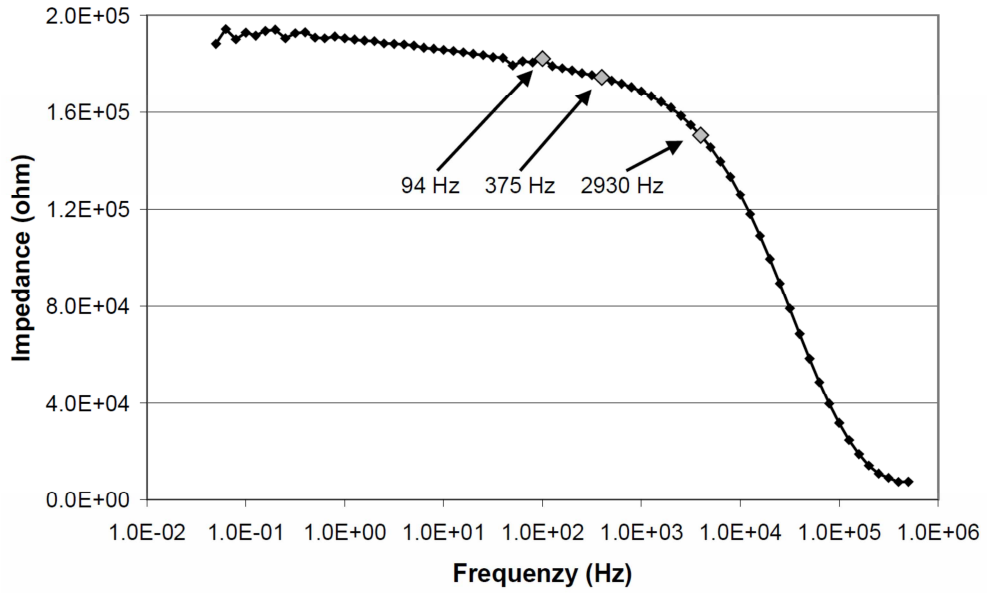

Figure 25. Impedance spectroscopy of Laxemar sample leached in deionised water. Reproduced from Löfgren (2001, Figure A5-15).

For a number of drill core samples from both Forsmark and Oskarshamn, the "rock resistivity" has been measured by direct current, as well as by alternating current at the frequencies 10, 100, and 2,000 Hz in Löfgren et al. (2009). When doing this, the rock samples have been saturated with solutions (either 0.05 or 0.1 M NaCl) of ionic strengths representative for the pore water encountered in situ. It would be more correct to say that the rock's impedance is measured when using alternating current, where the results are based on the potential drop over, and current running through, the sample. However, the terms resistance and resistivity have been used in Löfgren et al. (2009), also when measuring by AC up to frequencies of 2,000 Hz. Accordingly, it has been chosen to continue using this terminology in this chapter, and leave it to the reader to make the correction to impedance, when necessary.

The resulting resistivities for the nine rock samples used in Löfgren et al. (2009) are provided in Table 9 in Section 4.3, and are illustrated in Figure 26. As can be seen from the figure, while there is generally a significant drop in rock resistivity between DC (0 Hz) and AC at 10 Hz, by on average 15%, the drop between AC at 10 Hz and 2,000 Hz is smaller.

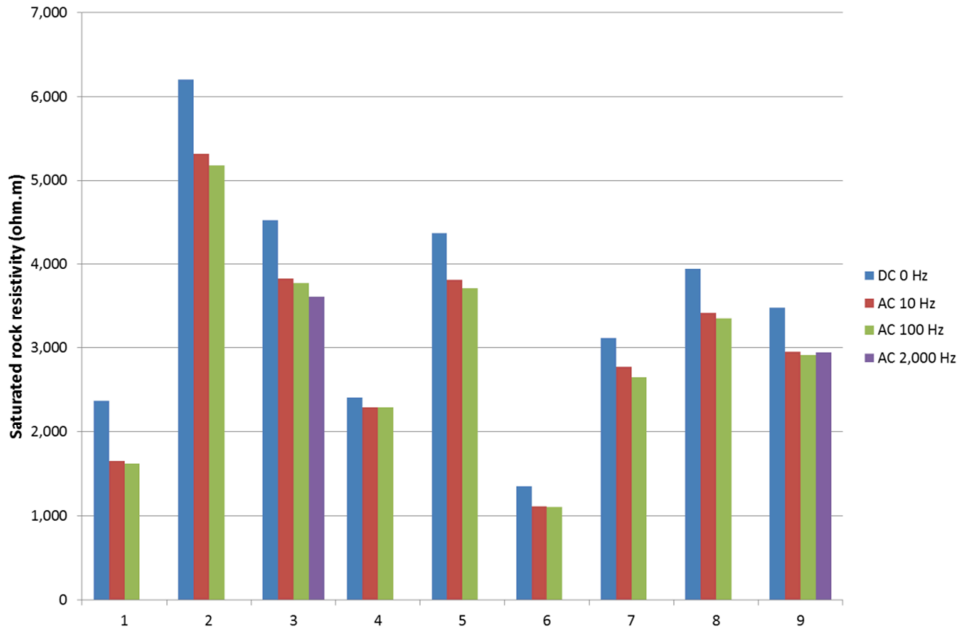

Figure 26. Saturated rock resistivities of nine Forsmark and Oskarshamn rock samples (cf. Table 9) at different frequencies. The saturation solution is 0.1 M NaCl for samples of odd numbers, and 0.05 M NaCl for samples of even numbers.

Very similar results have been obtained on three samples from the Äspö Hard Rock Laboratory (Vecernik et al. 2012, Table 3), where the drop between 0 Hz and 10 Hz on average is 19% and the average drop between 10 Hz and 2,000 Hz is 5%.

The rock resistivity of Sample 1 of Figure 26 has also been measured at DC and AC at the frequencies 10 and 100 Hz, when saturated with 0.001, 0.03, 0.05, and 1.0 M NaCl solutions (Löfgren et al. 2009). The data are provided in Table 10 in Section 5.2 and are illustrated in Figure 27.

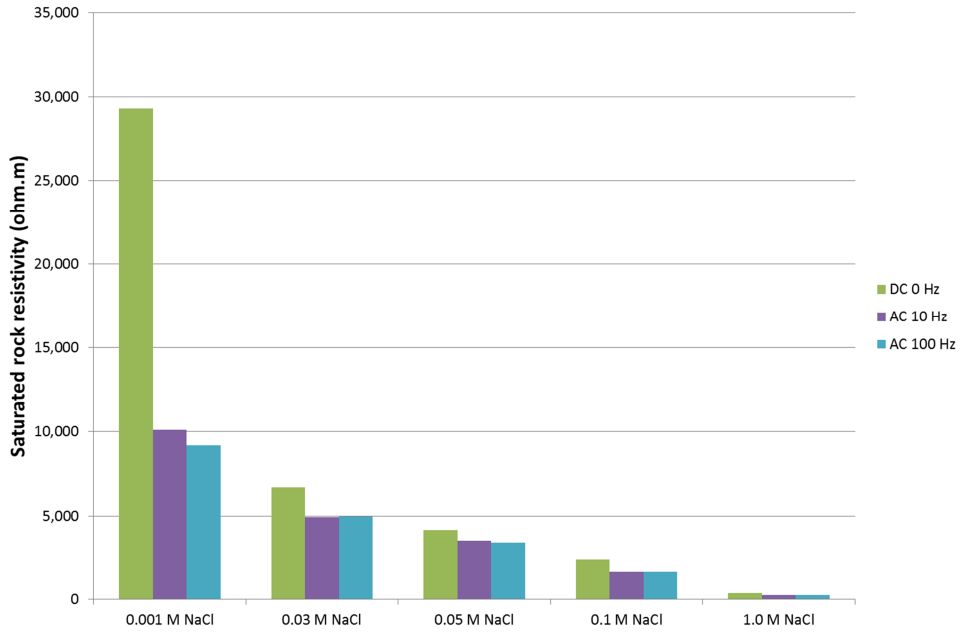

Figure 27. Saturated rock resistivities of a Sample 1 from Forsmark (cf. Table 10) at different frequencies, as saturated by different pore water solutions.

As can be seen in Figure 27, the relative drop in rock resistivity between 0 Hz and 10 Hz is much higher at low ionic strength than at high ionic strength. This is illustrated in a different way in Figure 28, where the saturated rock electrical conductivity is plotted versus the bulk pore electrical conductivity (EC), according to Equation 7. For the direct current results, this has already been plotted in Figure 14, but in Figure 28 the axes are in logarithmic scale to improve readability.

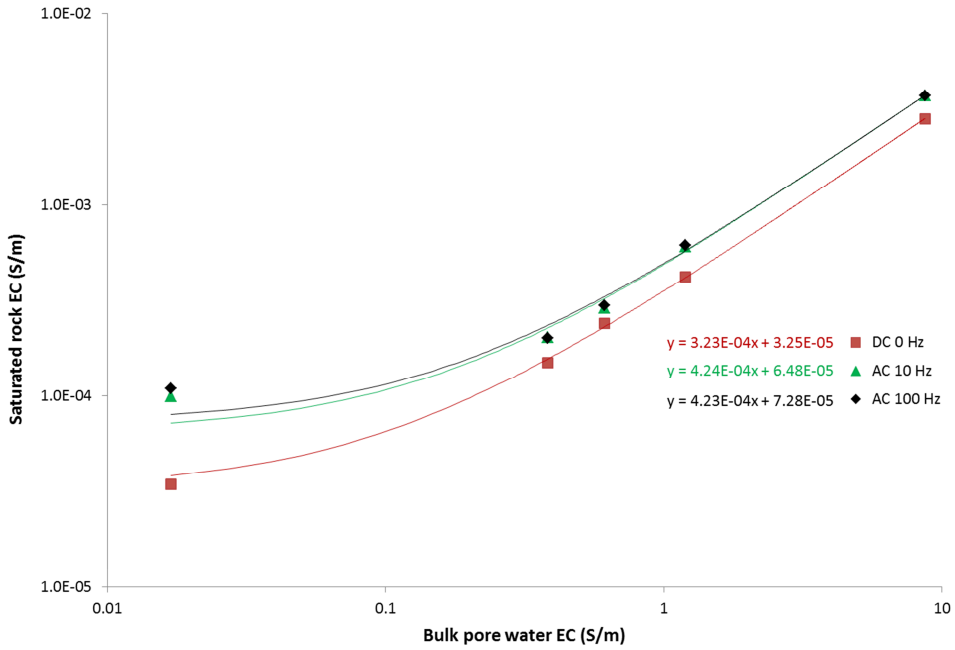

Figure 28. Saturated rock ECs of Sample 1 from Forsmark (cf. Table 10) at different frequencies, as saturated by pore water solutions of different EC. The fittings correspond to Equation 7.

As can be seen in Figure 28, the saturated rock electrical conductivity is overestimated when using alternating current (black and green curves) compared to using direct

current (red curve). This artefact is not corrected for by using Equation 9 and has, accordingly, not been corrected for in SR-Site. Judging from the fitting equations in Figure 28, using the slope to estimate the formation factor, the usage of alternating current at these frequencies will lead to an overestimated formation factor by a factor of 1.3. Moreover, from the intercept of the fittings it can be seen that when using alternating current at 100 Hz, this gives rise to an overestimation of the surface conductivity (compared to DC data) by a factor of 2.2.

6.4 Consequence for formation factor estimations in SR-Site

The estimation of the formation factor, and subsequently the effective diffusivity, has been done in two ways in SR-Site, as detailed in Chapter 3. One method relies directly on rock resistivity measurements in situ, performed at 2,000 Hz. The other method relies on effective diffusivities from laboratory through-diffusion measurements, but a correction factor has been applied for stress release and excavation induced damage. This correction factor is based on a comparison of in situ rock resistivities, obtained at 2,000 Hz, and laboratory resistivities, obtained at 0.1 Hz. In the comparison, the pore water electrical conductivity has been taken into account, together with the contribution from surface conduction (cf. Equation 9 in Section 5.3). This is further described in SKB (2010a, Section 6.8).

The first of the two methods suffers from the fact that a relatively high frequency has been used. According to Figure 26, using the impedance as a direct measure of the resistance would lead to an underestimation of the true rock resistivity by about 20%. This would on its own lead to an overestimation of the formation factor on about the same order of magnitude. On the other hand, Equation 9 has been used to make corrections for surface conduction. The constants in Equation 9 are in turn based on the fitting parameters of Figure 15. All but one data point in Figure 15 are based on alternating current measurements, using a frequency of around 100 Hz. Figure 28 indicates that when using alternating current at low ionic strength pore waters for measuring the surface conductivity, it is overestimated relative to the direct current surface conductivity by a factor of about two. This would mean that the fitting in Figure 15 is somewhat erroneous in its constants and that an over-correction has been made for surface conduction in SR-Site. It is reasonable to assume that this over-correction would, on its own, result in an underestimation of the formation factor (cf. calculation in Section 5.4) that is on the same order of magnitude as the overestimation induced by using 2,000 Hz in the in situ rock resistivity measurements. If so, errors stemming from the fact that alternating current have been used in the rock resistivity measurements would, roughly, cancel out.

In the second method, a correction factor for stress release and excavation induced damage is estimated by comparing the in situ and laboratory rock resistivities, both obtained by using alternating current. It appears that the difference in resistivity (impedance) is smaller when going from 0.1 Hz to 2,000 Hz, than when going from direct current to 2,000 Hz (cf. Figure 24 to Figure 26). Accordingly, the error evoked from this issue should be smaller than the ~20% deduced from Figure 26. The error evoked by using Equation 9, correcting for surface conduction, should be on the same order of magnitude as for the first method. If the error due to over-correcting for surface conduction is larger than that stemming from using different frequencies in the comparison, this would ultimately lead to a somewhat overestimated correction factor for stress release. If applying this somewhat overestimate correction factor on laboratory

formation factors, it would give somewhat underestimated in situ formation factors, which would be conservative from a radionuclide retention point of view.

In the above discussion, it is a prerequisite that there are no metallic minerals which blocks the pores. Such effects are instead discussed in the following chapter. Even under this prerequisite, it is noted that there are a few ifs and buts in the reasoning around the error evoked in the formation factor estimations when using alternating current. It is recognised that better knowledge on this matter would allow for more precise corrections. Relating to item 6 of SSM's request, concerning the uncertainty in the flowpath averaged formation factor, one can assume that the error induced from using alternating current is constrained within a factor of about two, based on available data. Overall, it is judged that the remaining errors/uncertainties are most likely too small to have a significant impact on the radionuclide transport results in SR-Site.

7 Investigating coupled electronic and electrolytic conduction and its influences on pore connectivity

7.1 Background and experimental data

As discussed in the above chapters, it is unlikely that long-range electronic conduction occurs in the rock matrix. However, it is conceivable that minerals allowing for electronic conduction on occasion block micropores and/or short-circuit nearby micropores. This may lead to a case where a direct electric current can pass through the blocking mineral, but where diffusing solutes cannot. If focusing on the blocking of micropores, this could have two main consequences for retention by matrix diffusion. Firstly, this could increase the tortuosity and constrictivity of the system, thus lowering the rock's formation factor and effective diffusivity. Secondly, if the blockage is pronounced enough, it could affect the connectivity of the porous system, only allowing for matrix diffusion into a finite volume of the rock matrix adjacent to the flowpath. Even if the porous system is not completely blocked, it has been hypothesized that porous systems at the percolation threshold can give rise to anomalous diffusion; also in rock types of concern for the Forsmark site (see overview in Haggerty (1999)). From a safety assessment point of view, at least if only taking radionuclide retention into account, limitations of the pore connectivity would be more detrimental than a decrease in effective diffusivity. This is as most retention occurs by sorption. For sorbing radionuclides, matrix diffusion contributes to their retention primarily by bringing them to the internal mineral surfaces of the rock matrix where they can sorb. If the connectivity of the microporous system would be severely limited, only a relatively small part of the rock matrix's inner surfaces would become available for sorption.

In this report, mineral grains allowing for electronic conduction are generally assumed to be metallic in nature, even if there are difficulties involved in discriminating metallic from non-metallic minerals. Here it should be reminded that metallic minerals are not in their pure metallic form (cf. Section 6.1) and that they, in general, pose a low resistance to electronic conduction. If looking at the resistivity of the perceived metallic mineral magnetite in Table 6, one can see that it is reported to range from $5 \cdot 10^{-5} – 5.7 \cdot 10^{3}$ ohm.m. Compared to the intrinsic resistivity of the pore water, which is around 1 ohm.m, magnetite grains at the lower end of this range would allow for the short-circuiting effect discussed in this chapter, while there would be poor short-circuiting due to magnetite grains at the upper end of the resistivity range. On this account, it is difficult to say that a certain mineral is of importance for coupled electronic and electrolytic conduction. For the purpose of this report, a mineral is called metallic when:

1. the mineral has a resistivity close to that of the pore water (1 ohm.m), or lower,
2. the mineral surface can undergo electrochemical reactions, facilitating the transfer of electrolytic conduction to electronic conduction, and vice versa.

About a decade ago, the so called through-electromigration (TEM) method (Löfgren 2004) was developed with the primary aim to investigate if metallic minerals can block pores and restrict the migration of solutes, but still allow for direct electric current to pass. The equipment involved in the method, as well as its performance, is described in detail in Löfgren (2004), Löfgren and Neretnieks (2006), Löfgren et al. (2009) and

Vecernik et al. (2012). As for the other electrical methods, TEM relies on the Einstein relation between electromigration and diffusion (as incorporated in Equation 10). Solute migration occurs with an electrical potential gradient as the main driving force, using direct current. However, apart from other electrical methods, in a TEM experiment an ionic tracer is allowed to electromigrate through the rock sample and a breakthrough curve can be obtained. An example of such a breakthrough curve is shown in Figure 29.

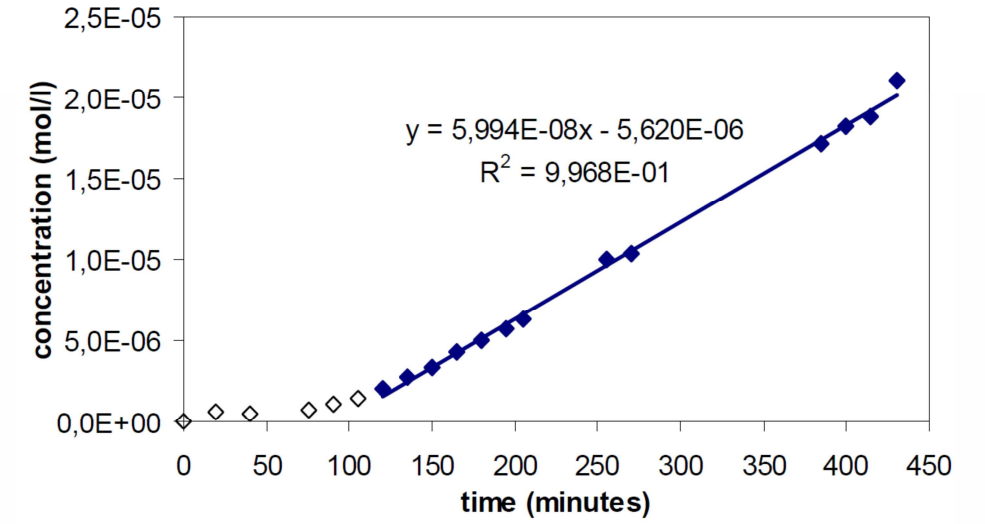

Figure 29. TEM experiment: Iodide breakthrough curve for sample AD-1 (10 mm length). Full diamonds represent steady state conditions. Tracer injection occurs at 0 minutes. Figure reproduced from Vecernik et al. (2012, Figure 6).

The effective diffusivity D_e (m^2/s) can be calculated directly from the electromigratory flux N_μ ($mol/m^2.s$) into the low concentration tracer cell, which in turn determines the slope of the steady state part of the breakthrough curve:

$$N_\mu = -\frac{FzD_e}{RT} C_p \frac{dU}{dx} \qquad \text{Equation 10}$$

where C_p (mol/m^3) is the tracer concentration in the high concentration cell, dU/dx (V/m) is the potential gradient over the rock sample, and F, R, and T are the gas constant, temperature, and Faraday constant, respectively. Equation 10 is derived in Löfgren et al. (2009, Chapter 3).

One interesting feature of the TEM method is that the pore connectivity can be demonstrated in samples long enough to make similar measurements with diffusive methods very time consuming. In Löfgren and Neretnieks (2006), the tracer was driven through samples up to 121 mm in length, at rates reasonably well predicted by effective diffusivities obtained in through-diffusion experiments on adjacent, but much shorter, drill core samples. From these experiments, performed on samples from the borehole KLX02 in Laxemar, there was no sign of significant blocking of pores by conductive minerals, at least not on the decimetre-scale and at stress released conditions. If there was significant blockage of the pores, this would have been demonstrated either by a no-show of tracers, or a much reduced flux of tracers through the long samples. For reference, numerical data of the resulting formation factors are tabulated in Appendix B, and the data are displayed in Figure 30.

Simultaneously as running the TEM experiment, direct current formation factor measurements can be carried out. As discussed in the above chapters, the formation

factor is derived from measurements of the saturated rock resistivity, the electrical conductivity of the electrolyte the rock is saturated with, and by making the correction for surface conduction. By converting the effective diffusivity derived from the TEM breakthrough curve to the formation factor, it can be compared with that obtained from the direct current resistivity method. This has been done on nine Forsmark and Oskarshamn samples in Löfgren et al. (2009), three Äspö samples in Vecernik et al. (2012) and eight Laxemar samples in Löfgren and Neretnieks (2006). Numerical data are tabulated in Appendix B, and the data are displayed in Figure 30. In the original references the apparent formation factor has been reported. By using Equation 9, the formation factor has been estimated in this present report.

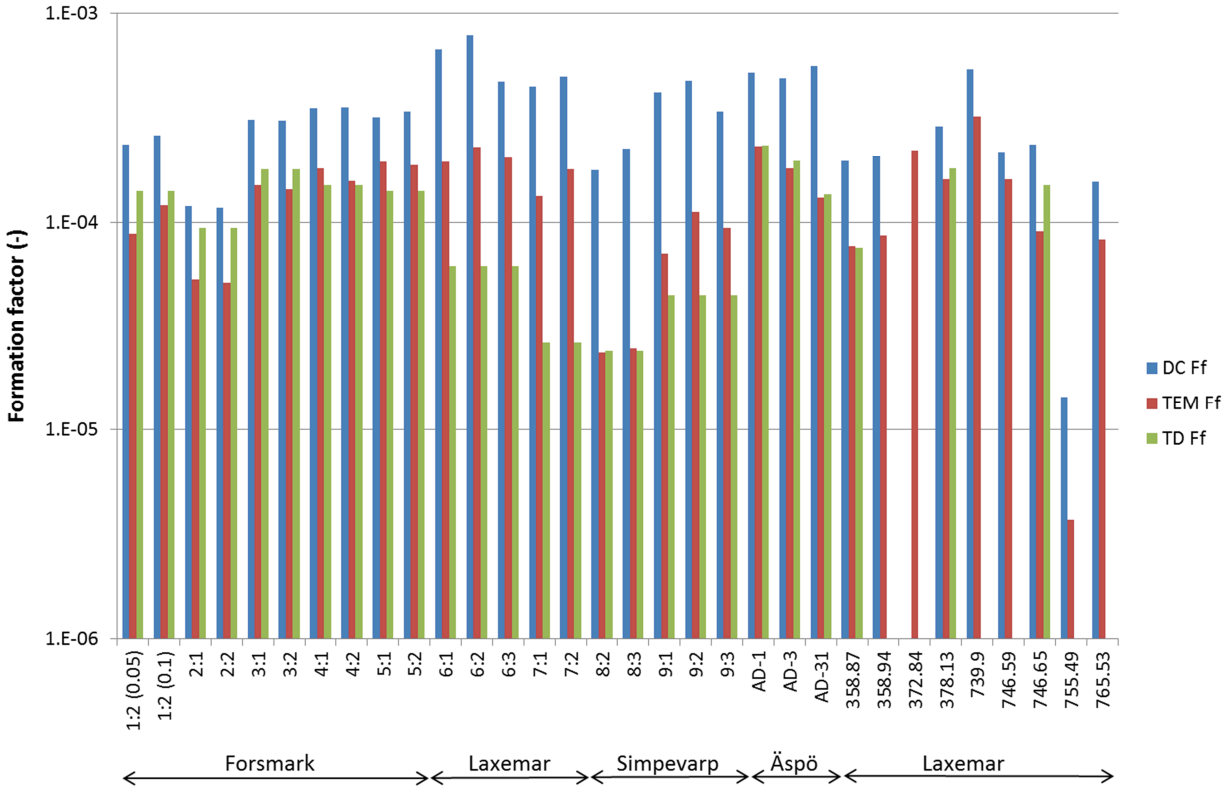

Figure 30. Formation factors obtained by the through-electromigration method, using the anionic tracer iodide, the through-diffusion (TD) method, and the DC rock resistivity method. Data are based on Löfgren (2004), Löfgren and Neretnieks (2006), Löfgren et al. (2009) and Vecernik et al. (2012). Sample labelling is explained in Appendix B.

In the TEM measurements, the anionic tracer iodide has been used. Using an anionic tracer, subjected to anion exclusion, and not also cationic tracers somewhat complicates the comparison with DC results. This is as the direct current utilises both cations and anions. From this, one can expect that the DC formation factor is somewhat larger than the TEM formation factor. Unfortunately, if there were metallic minerals blocking part of the pores, allowing for the passing of electric current but not the passing of solutes, this could manifest in the same way when ultimately estimating the formation factor.

As can be seen in Figure 30, the DC formation factors (blue bars) are systematically larger than the TEM formation factors (red bars). In Figure 31 the ratios of the DC, TEM and through-diffusion (TD) formation factors are given, for the Forsmark samples of Löfgren et al. (2009).

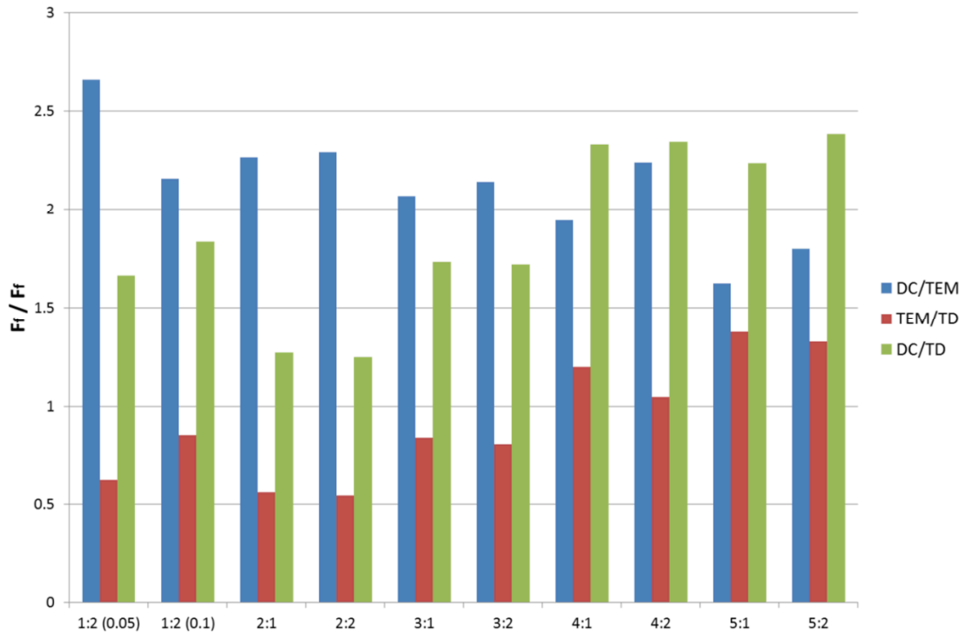

Figure 31. Ratios of the DC, TEM and through- diffusion (TD) formation factors, for the Forsmark samples of Löfgren et al. (2009).

As can be seen in Figure 31, the DC/TEM formation factor ratio is in the range 1.6 to 2.7, which may indicate general anion exclusion or, perhaps, blocking of micropores. When looking at the TEM/TD formation factor ratio it varies within the range of 0.54 to 1.4. Accordingly, no general anion exclusion can be deduced from these data. On the other hand, it should be reminded that there could be biases between the methodologically very different methods that could mask such an effect, considering the relatively small differences in the results. The DC/TD ratio is in the range 1.2 to 2.4, which could also indicate limited blocking of the micropores.

As seen in Figure 31, the ratios are reasonably close to unity. However, if comparing the formation factors from the Oskarshamn site (sample number 6:1 to AD-31 in Figure 30) obtained by different methods in Löfgren et al. (2009) and Vecernik et al. (2012), they differ to a larger degree. One may speculate that the short sample length (~10 mm) in combination with the Oskarshamn rock types can offer an explanation. If so, short circuiting of nearby micropores by metallic minerals, or perhaps sheet silicates such as biotite, is a more likely explanation than blockage of pores. When increasing the sample length, (cf. sample 358.87 to 765.53) the situation resembles that of Figure 31, also for the Laxemar samples.

7.2 Consequence for formation factor estimations in SR-Site

In conclusion, information from the through-electromigration experiments so far tells different stories. In Löfgren and Neretnieks (2006) no sign of significantly reduced connectivity was shown, as result of metallic minerals blocking the pores, even for longer samples. However, based on all experiments performed up to date, the formation factor estimated by direct current measurements generally seems to be somewhat higher than when obtained in through-diffusion measurements. There may be a plenitude of

explanations for this that would not include the blockage of micropores by metallic minerals. Such explanations range from questioning the applicability of the fundamental theories in crystalline rock, to the presence of non-metallic mineral occupying the pores. Relating to the former issue, Fick's laws and the Einstein relation were not intended for use in the highly charged system of crystalline rock. Relating to the latter issue, clay minerals have been found to occupy pores and while such minerals would allow for the passing of an electrical current, as well as for the passing of non-charged species and cations, they would hinder anion migration. On this account, one may expect a discrepancy when comparing TEM formation factors, using iodide as the tracer, and DC formation factors.

If there was severe blocking of the pores, the passing of an electric current would require numerous of transitions from electrolytic to electronic conduction, and vice versa. Each of these transitions would be associated with a reaction, and this would decrease the efficiency of the current propagation. As stated in Section 6.1 this would be similar to ohmic dissipation, and would result in a significantly increased saturated rock resistivity. This has not been observed and, accordingly, one can assume that if metallic minerals at all block micropores, the blocking would be limited. Providing that the deviation between formation factors estimated by tracer tests and electrical methods stays within the range displayed in Figure 31, the uncertainty induced by this artefact is comparable with other uncertainties induced in matrix diffusion estimates, and should be of little concern for the safety assessment. However, as long as there is a risk of processes/features that even further lower the already low effective diffusivity suggested in SR-Site, or suggest limitations in the pore connectivity, the matter deserves more attention. As there is a certain lack in understanding associated with electrical methods, it is wise to base the prediction of matrix diffusion on a range of experimental observations, including those from in situ diffusion experiments. This approach has also been taken in SR-Site.

Relating to item 6 of SSM's request, concerning the uncertainty in the flowpath averaged formation factor, it seems that the use of electrical current may lead to overestimated formation factors, compared to when using tracer tests (cf. the DC/TD ratio of Figure 31). On average, the induced uncertainty is estimated to be a factor of about two for Forsmark rock.

8 Conclusions

8.1 General knowledge

In conclusion, new and highly interesting information has emerged on the rock matrix diffusivity over the past decade from using electrical methods within the SKB research programme. The perhaps most controversial result is the clear indication that experiments performed in the laboratory may overestimate the effective diffusivity by about an order of magnitude. This is generally ascribed to the stress release and/or excavation induced damage that the laboratory samples are subjected to. If this result is accurate, it would evoke a need to further pursue in situ investigations of rock that remains under the natural stress conditions and is not subjected to excavation damage.

From a radionuclide retention point of view, it would be non-conservative to disregard the indications of decreased in situ effective diffusivities, compared to those measured in the laboratory. Accordingly, information from the electrical in situ measurements has been given much weight when estimating the effective diffusivity in SR-Site, even if the electrical method is less mature, and may be associated with more artefacts, than the laboratory diffusion methods normally used within the scientific community.

In this report, the impacts of some known artefacts associated with electrical methods have been quantified as far as possible. Discussed artefacts are (in order of appearance):

1. Long-range electronic conduction in the mineral lattices.
2. Surface conduction.
3. Dielectric effects, stemming from using alternating current.
4. Short-range electronic conduction in metallic minerals blocking the micropores.

Concerning the first artefact, it is concluded that such long-range electronic conduction does not occur at Forsmark. This statement is based on recently performed dry rock resistivity measurements, and a study of abundant minerals and fracture minerals at Forsmark. By looking at the abundances, and literature values of the minerals' intrinsic resistivities, the notion that long-range electronic conduction would be of any importance at Forsmark can be rejected.

The errors associated with the second and third artefacts have their basis in the fact that the typical mineral grains at Forsmark are negatively charged, which affects the ionic solutes in the pore water. One may venture to say that the errors associated with these artefacts are reasonably well constrained, even if more testing is needed to further reduce data uncertainty. Data indicate that the magnitude of the errors is only weakly associated with minor deviations in the mineral composition.

Errors associated with the fourth artefact are more difficult to constrain. Here it is postulated that metallic minerals may block micropores. Such blocking minerals may hinder solute transport but allow for an electric current to pass. In geophysical literature (e.g. Telford et al. 1990), it is clearly stated that the presence of metallic minerals should be detected by an increased phase angle. However, only very few samples from Forsmark show increased phase angles (cf. Figure 22). On the other hand, there is a discrepancy between formation factors obtained with DC measurements, eliminating dielectric artefacts, and those obtained by tracer tests. One explanation for this, out of many, could be metallic minerals blocking the micropores, at least to a limited extent.

Concerning the pore connectivity, it was suggested to be sufficient for all scales of interest for the safety assessment in SR-Site (SKB 2010a, Section 6.8). Long-range pore connectivity was also argued for in SKB (2010c, Section 5.3). After taking the additional information of this present report into consideration, no argument has been found that counteracts the notion of long-range connectivity. Within the scientific community, this notion has gained momentum over the last decade or so, based on empirical evidences from in situ diffusion tests and impregnations. Concerning the in situ electrical method presently used by SKB, the fact that current can be propagated into the rock matrix provides additional support to the notion of long-range pore connectivity, although the support may be considered as weak as alternating current is used. Injecting direct current into the non-fractured rock matrix in situ would be beneficial for the case of demonstrating long-range pore connectivity. Utilising long-range electromigration methods in situ, allowing for tracers to electromigrate a metre or so into the rock matrix, may ultimately prove the case. However, such experiments exist only in a premature planning state and would, by necessity, be performed from tunnels which are not yet built at the Forsmark site.

8.2 Consequence for SR-Site

Based on the considerations provided in this report, the expert judgment is still that the data delivered to SR-Site on formation factors and effective diffusivities are reasonable. In hindsight one can question the usage of a single point value for the formation factor, as justified by the fact that flowpath averaged values should be used in subsequent radionuclide transport modelling. The biases discussed in this report will not be flowpath averaged, even though some will partly cancel out. There are also some uncertainties concerning the estimates of the in situ pore water electrical conductivity, discussed in Crawford (2012), which may give rise to minor bias. Accordingly, in future safety assessments, it is advised against using a single point value for the flowpath averaged formation factor, if such high degree of resolution is required in input data. As elaborated on in Sections 6.4, the uncertainty/bias originating from the fact that alternating current is used in situ should be constrained within a factor of two. As elaborated on in Sections 7.2, the uncertainty/bias originating in the fact that (direct) electric current is used, as opposed to using tracers, should on average be a factor of about two.

Considering the gaps in scientific knowledge on a number of issues, making a formal error propagation of the bias in the flowpath averaged in situ formation factor would not be justifiable. However, based on the information provided in this report, it seems likely that the "true" flowpath averaged in situ formation factor has a value close to $2.1 \cdot 10^{-5}$, as stated in SR-Site (SKB 2010a, Section 6.8). Here it should be highlighted that this value corresponds to the undisturbed rock, and not necessarily is valid for the altered/disturbed rock matrix directly adjacent to the flowpath.

If speaking in terms of logarithmic values, $\log_{10}(2.1 \cdot 10^{-5})$ equals –4.68. It seems likely that the "true" flowpath averaged in situ formation factor is located within half an order of magnitude of $(\log_{10}F_f) = -4.68$. If attempting to describe the resulting bias in a probabilistic distribution, for possible use in stochastic safety assessment modelling, one may assume that the uncertainty associated with the bias is log-normally distributed. Furthermore, one may say that there is a 95% probability of finding the "true" flowpath averaged in situ formation factor within half an order of magnitude from $(\log_{10}F_f) = -4.68$. This would give rise to a log-normal distribution for the

flowpath averaged formation factor where $\mu(\log_{10}F_f) = -4.68$ and $\sigma(\log_{10}F_f) = 0.25$. Here, μ and σ signify the mean and standard deviation of the distribution.

In another report by Löfgren and Crawford (2014), also responding to SSM's requests for supplementary information (SSM 2013), a layered rock matrix model is used in radionuclide retention calculations. Here, the rock matrix directly adjacent to flowpaths is assigned an increased porosity and formation factor, compared to the underlying undisturbed rock. If including data for fracture minerals and the alteration rim in the formation factor uncertainty range, it would become much larger than what is suggested in this present report. Also, the mean value of the formation factor would be significantly shifted upwards. Accordingly, the impact of the SR-Site decision to rely on data for the undisturbed rock when modelling retention by matrix diffusion overshadows the impact of the uncertainty in the flowpath averaged in situ formation factor discussed in the present report.

Generally the uncertainties associated with the formation factor and effective diffusivity estimates, performed as part of SR-Site, are judged to be too small to impact the radionuclide transport modelling to a significant degree. If there would be a noticeable impact, it would be on the conservative side in relation to radionuclide retention, as result of the SR-Site decision to neglect the increased matrix diffusion in the alteration rim of flowpath adjacent rock. Therefore, it can be concluded that the formation factor and effective diffusivity have been sufficiently well estimated to fulfil the requirements of radionuclide transport modelling in the SR-Site safety assessment.

References

Aalto P, Aaltonen I, Kemppainen K, Koskinen L, Lahti M, Lindgren S, Mustonen A, Ylä-Mella M, Ahokas H, Hellä P, Andersson J, Hakala M, Hudson J, Johansson E, Snellman M, Laaksoharju M, Pedersen K, Pitkänen P, Poteri A, 2009. Programme for repository host rock characterisation in the ONKALO (ReRoC). Posiva Working Report 2009-31, Posiva Oy, Finland.

Archie G E, 1942. The electrical resistivity log as an aid in determining some reservoir characteristics. Petroleum Transactions of AIME 146, 54–62.

Brace W F, Orange A S, 1968. Further studies of the effects of pressure on electrical resistivity of rocks. Journal of Geophysical Research 73, 5407–5420.

Brace W F, Orange A S, Madden T R, 1965. The effect of pressure on the electrical resistivity of water-saturated crystalline rocks. Journal of Geophysical Research 70, 5669–5678.

Byegård J, Selnert E, Tullborg E-L, 2008. Bedrock transport properties. Data evaluation and retardation model. Site descriptive modelling, SDM-Site Forsmark. SKB R-08-98, Svensk Kärnbränslehantering AB.

Crawford J (ed), 2008. Bedrock transport properties Forsmark. Site descriptive modelling, SDM-Site Forsmark. SKB R-08-48, Svensk Kärnbränslehantering AB.

Crawford J, 2010. Bedrock K_d data and uncertainty assessment for application in SR-Site geosphere transport calculations. SKB R-10-48, Svensk Kärnbränslehantering AB.

Crawford J, 2012. Decreasing uncertainty of radionuclide migration predictions in safety assessment modeling. In Rabung T, Molinero J, Garcia D, Montoya V (eds). 1st Workshop Proceedings of the Collaborative Project "Crystalline Rock Retention Processes" (7th EC FP CP CROCK). Karlsruhe: KIT Scientific Publishing. (KIT Scientific Reports 7629), 73–95.

Crawford J, Sidborn M (eds), 2009. Bedrock transport properties Laxemar. Site descriptive modelling, SDM-Site Laxemar. SKB R-08-94, Svensk Kärnbränslehantering AB.

Dakhnov V N, 1962. Geophysical well logging: the application of geophysical methods: electrical well logging. Quaterly of the Colorado School of Mines 57:2.

Drake H, Sandström B, Tullborg E-L, 2006. Mineralogy and geochemistry of rocks and fracture fillings from Forsmark and Oskarshamn: Compilation of data for SR-Can. SKB R-06-109, Svensk Kärnbränslehantering AB.

Eklund S, Mattsson K-J, 2009. Forsmark site investigation. Quantitative mapping of fracture minerals in Forsmark. SKB P-08-47, Svensk Kärnbränslehantering AB.

Haggerty R, 1999. Application of the multirate diffusion approach in tracer test studies at Äspö HRL. SKB R-99-62, Svensk Kärnbränslehantering AB.

Haggerty R, 2012. Review of matrix diffusion and related properties of intact rock in SKB's licence application for a spent nuclear fuel repository in Forsmark, Sweden. Technical Note 2012:44, Strålsäkerhetsmyndigheten (Swedish Radiation Safety Authority).

Keller G V, Frischknecht F C, 1966. Electrical methods in geophysical prospecting. Oxford: Pergamon.

Löfgren M, 2001. Formation factor logging in igneous rock by electrical methods. Lic. thesis. Royal Institute of Technology, Stockholm, Sweden.

Löfgren M, 2004. Diffusive properties of granitic rock as measured by in situ electrical methods. PhD thesis. Department of Chemical Engineering and Technology, Royal Institute of Technology, Stockholm, Sweden.

Löfgren M, 2007. Forsmark site investigation. Formation factor logging in situ by electrical methods in KFM01D and KFM08C. SKB P-07-138, Svensk Kärnbränslehantering AB.

Löfgren M, Crawford J, 2014. Modelling of radionuclide retention by matrix diffusion in a layered rock model. Response to the request by SSM for supplementary information on retention of radionuclides (SSM2011-2426-110), items 4 and 6 (SKBdoc 1421960).

Löfgren M, Neretnieks I, 2006. Through-electromigration: a new method of investigating pore connectivity and obtaining formation factors. Journal of Contaminant Hydrology 87, 273–252.

Löfgren M, Sidborn M, 2010. Statistical analysis of results from the quantitative mapping of fracture minerals in Forsmark. Site descriptive modelling – complementary studies. SKB R-09-30, Svensk Kärnbränslehantering AB.

Löfgren M, Pettersson M, Widén H, Crawford J, 2006. Forsmark site investigation. Formation factor logging in-situ by electrical methods in KFM05A and KFM06A. SKB P-06-91, Svensk Kärnbränslehantering AB.

Löfgren M, Večernik P, Havlova V, 2009. Studying the influence of pore water electrical conductivity on the formation factor, as estimated based on electrical methods. SKB R-09-57, Svensk Kärnbränslehantering AB.

Neretnieks I, 1980. Diffusion in the rock matrix: an important factor in radionuclide retardation? Journal of Geophysical Research 85, 4379–4397.

Nilsson K, Bergelin A, Lindquist A, Nilsson A-C, 2006. Forsmark site investigation. Hydrochemical characterisation in borehole KFM01D. Results from seven investigated borehole sections: 194.0–195.0 m, 263.8–264.8 m, 314.5–319.5 m, 354.9–355.9 m, 369.0–370.0 m, 428.5–435.6 m, 568.0–575.1 m. SKB P-06-227, Svensk Kärnbränslehantering AB.

Ohlsson Y, 2000. Studies of ionic diffusion in crystalline rock. PhD thesis. Royal Institute of Technology, Stockholm, Sweden.

Ohlsson Y, Neretnieks I, 1998. Some evidence for surface ion mobility in rock. Journal of Contaminant Hydrology 35, 91–100.

Olin M, M Valkiainen, H Aalto, 1997. Matrix diffusion in crystalline rocks: coupling of anion exclusion, surface diffusion and surface complexation. Posiva 96-25, Posiva Oy, Finland.

Revil A, Glover P W J, 1997. Theory of ionic-surface electrical conduction in porous media. Physical Review B 55, 1757–1773.

Sandström B, Stephens M B, 2009. Mineralogy, geochemistry, porosity and redox properties of rocks from Forsmark. Compilation of data from the regional model volume for SR-Site. SKB R-09-51, Svensk Kärnbränslehantering AB.

Schön J H, 1996. Physical properties of rock: fundamentals and principles of petrophysics. Oxford: Pergamon.

Selnert E, Byegård J, Widestrand H, 2008. Forsmark site investigation. Laboratory measurements within the site investigation programme for the transport properties of the rock. Final report. SKB P-07-139, Svensk Kärnbränslehantering AB.

Selnert E, Byegård J, Widestrand H, 2009. Oskarshamn site investigation. Laboratory measurements within the site investigation programme for the transport properties of the rock. Final report. SKB P-07-179, Svensk Kärnbränslehantering AB.

Siitari-Kauppi M, Ikonen J, Kauppi L, Lindberg A, 2010. Investigation of porosity and pore structure adjacent to fractures by PMMA method; Samples taken from drill cores at Olkiluoto. Posiva Working Report 2010-66, Posiva Oy, Finland.

Skagius K, Neretnieks I, 1983. Diffusion measurements in crystalline rocks. SKBF/KBS TR 83-15, Svensk Kärnbränsleförsörjning AB.

Skagius K, Neretnieks I, 1986. Diffusivity measurements and electrical resistivity measurements in rock samples under mechanical stress. Water Resources Research 22, 570–580.

SKB, 2008. Site description of Forsmark at completion of the site investigation phase. SDM-Site Forsmark. SKB TR-08-05, Svensk Kärnbränslehantering AB.

SKB, 2010a. Data report for the safety assessment SR-Site. SKB TR-10-52, Svensk Kärnbränslehantering AB.

SKB, 2010b. Comparative analysis of safety related site characteristics. SKB TR-10-54, Svensk Kärnbränslehantering AB.

SKB, 2010c. Geosphere process report for the safety assessment SR-Site. SKB TR-10-48, Svensk Kärnbränslehantering AB.

SKB, 2010d. Model summary report for the safety assessment SR-Site. SKB TR-10-51, Svensk Kärnbränslehantering AB.

SKB, 2011. Long-term safety for the final repository for spent nuclear fuel at Forsmark. Main report of the SR-Site project. SKB TR-11-01, Svensk Kärnbränslehantering AB.

SSM, 2013. Begäran om komplettering av ansökan om slutförvaring av använt kärnbränsle och kärnavfall – Retardation av radionuklider. SSM2011-2426-110, Strålsäkerhetsmyndigheten (Swedish Radiation Safety Authority). (In Swedish.)

Stumm W, Morgan J J, 1996. Aquatic chemistry: chemical equilibria and rates in natural waters. 3rd ed. New York: Wiley.

Telford W M, Geldart L P, Sheriff R E, 1990. Applied geophysics. 2nd ed. Cambridge: Cambridge University Press.

Thunehed H, 2007a. Oskarshamn site investigation. Resistivity measurements on samples from KSH01, KSH02, KLX02, KLX04 and KLX11A. SKB P-06-289, Svensk Kärnbränslehantering AB.

Thunehed H, 2007b. Forsmark site investigation. Resistivity measurements on samples from KFM01A, KFM01B, KFM02A, KFM05A and KFM06A. SKB P-07-51, Svensk Kärnbränslehantering AB.

Thunehed H, 2007c. Forsmark site investigation. Complementary resistivity measurements on samples from KFM01A, KFM02A, KFM06A, KFM08A, KFM08C and KFM09A. SKB P-07-137, Svensk Kärnbränslehantering AB.

Thunehed H, 2007d. Oskarshamn site investigation. Complementary resistivity measurements on samples from KLX03, KLX04, KLX05, KLX10, KLX12A and KLX13A. SKB P-07-203, Svensk Kärnbränslehantering AB.

Tsuda N, Nasu K, Fujimori A, Siratori K, 2000. Electronic conduction in oxides. 2nd ed. Berlin: Springer. (Springer Series in Solid-State Sciences 94).

van Olphen H, Waxman M H, 1956. Surface conductance of sodium bentonite in water. Clays and Clay Minerals 5, 61–80.

Vecernik P, Havlova V, Löfgren M, 2012. Determination of rock migration parameters (F_f, D_e): application of electromigration method on samples of different length. In Rabung T, Molinero J, Garcia D, Montoya V (eds). 1st Workshop Proceedings of the Collaborative Project "Crystalline Rock Retention Processes" (7th EC FP CP CROCK). Karlsruhe: KIT Scientific Publishing. (KIT Scientific Reports 7629), 137–147.

Väisäsvaara J, Leppänen H, Pekkanen J, 2006. Forsmark site investigation. Difference flow logging in borehole KFM01D. SKB P-06-161, Svensk Kärnbränslehantering AB.

Waber H N, Smellie J A T, 2005. Forsmark site investigation. Borehole KFM06A: Characterisation of pore water. Part 1: Diffusion experiments. SKB P-05-196, Svensk Kärnbränslehantering AB.

Waxman M H, Smits L J M, 1968. Electrical conductivities in oil-bearing shaly sands. Society of Petroleum Engineering Journal 8, 107–122.

Appendices

Appendix A

Raw data on which averaged values in Table 9 and Table 10 are based. Data reproduced from Löfgren et al. (2009, Appendices A and B).

	Sample 2, KFM01A 312.54		**Sample 3, KFM02A 554.60**		**Sample 4, KFM01A 554.71**		**Sample 5, KFM02A 554.84**	
	0.1 M 1st run	0.1 M 2nd run	0.05 M 1st run	0.05 M 2nd run	0.1 M 1st run	0.1 M 2nd run	0.05 M 1st run	0.05 M 2nd run
Water EC	1.14	1.11	0.586	0.584	1.06	1.05	0.575	0.569
DC	6087	6326	4493	4536	2411	2418	4473	4260
AC 10 Hz	5274	5353	3798	3852	2290	2310	3707	3910
AC 100 Hz	5135	5225	3747	3790	2331	2264	3665	3759
AC 2000 Hz			3597	3629				
TD F_f	9.39E-04		1.78E-04		1.50E-04		1.41E-04	

	Sample 6, KLX04 489.49			**Sample 7, KLX04 489.61**	
	0.1 M 1st run	0.1 M 2nd run	0.1 M 3rd run	0.05 M 1st run	0.05 M 2nd run
Water EC	1.15	1.15	1.07	0.584	0.577
DC	1201	1038	1815	3256	2972
AC 10 Hz	1220	1062	1050	2783	2766
AC 100 Hz	1190	1047	1079	2665	2641
AC 2000 Hz					2602
TD F_f	6.13E-05			2.63E-05	

	Sample 8, KSH02 474.47			**Sample 9, KSH02 474.66**		
	0.1 M 1st run	0.1 M 2nd run	0.1 M 3rd run	0.05 M 1st run	0.05 M 2nd run	0.05 M 3rd run
Water EC	~1[a]	1.148	1.064	0.574	0.579	0.635
DC	4700	4255	3632	3493	3081	3879
AC 10 Hz		3703	3138	2940	2704	3208
AC 100 Hz		3579	3108	2913	2666	3154
AC 2000 Hz				3068	2781	2981
TD F_f	2.39E-05			4.46E-05		

a) Not measured
Units: Water EC (S/m), DC (ohm.m), AC 10 Hz (ohm.m), AC 100 Hz (ohm.m), AC 2000 Hz (ohm.m), TD F_f (–)
All electrolytes are NaCl solutions of different concentrations.

Sample 1, KFM01A 312.66-312.67

	0.001 M 1st run	0.001 M 2nd run	0.03 M 1st run	0.03 M 2nd run	0.03 M 3rd run	
Water EC	0.0114	0.0224	0.378	0.378	0.391	
DC	27557	31004	5469	9460	5140	
AC 10 Hz	13364	6871	1577	7059	6174	
AC 100 Hz	11622	6733	2029	6882	5984	
TD Ff	1.41E-04					
	0.05 M 1st run	0.05 M 2nd run	0.1 M 1st run	0.1 M 2nd run	1.0 M 1st run	1.0 M 2nd run
Water EC	0.578	0.6495	1.10	1.29	8.495	8.87
DC	3073	5268	2072	2682	312	393
AC 10 Hz	2643	4284	1792	1506	217	317
AC 100 Hz	2576	4125	1726	1509	221	313

Units: Water EC (S/m), DC (ohm.m), AC 10 Hz (ohm.m), AC 100 Hz (ohm.m), AC 2000 Hz (ohm.m), TD F_f (–)
All electrolytes are NaCl solutions of different concentrations.

Appendix B

Raw data behind Figure 26, Figure 27, Figure 30, and Figure 31.

Sample	Length (mm)	Pore water	Pore water EC (S/m)	DC F_f^{app} (-)	DC F_f (-)	TEM F_f (-)	TD F_f (-)	DC F_f / TEM F_f	DC F_f / TD F_f	TEM F_f / TD F_f
1:2 (0.05)	10	0.05 M	0.65	2.9E-04	2.3E-04	8.8E-05	1.4E-04	2.7	1.7	0.62
1:2 (0.1)	10	0.1 M	1.3	2.9E-04	2.6E-04	1.2E-04	1.4E-04	2.2	1.8	0.85
2:1	10	0.1 M	1.1	1.4E-04	1.2E-04	5.3E-05	9.4E-05	2.3	1.3	0.56
2:2	10	0.1 M	1.1	1.4E-04	1.2E-04	5.1E-05	9.4E-05	2.3	1.2	0.54
3:1	13	0.05 M	0.59	3.8E-04	3.1E-04	1.5E-04	1.8E-04	2.1	1.7	0.84
3:2	13	0.05 M	0.58	3.8E-04	3.1E-04	1.4E-04	1.8E-04	2.1	1.7	0.80
4:1	12	0.1 M	1.1	3.9E-04	3.5E-04	1.8E-04	1.5E-04	1.9	2.3	1.2
4:2	12	0.1 M	1.1	3.9E-04	3.5E-04	1.6E-04	1.5E-04	2.2	2.3	1.0
5:1	11	0.05 M	0.58	3.9E-04	3.2E-04	1.9E-04	1.4E-04	1.6	2.2	1.4
5:2	11	0.05 M	0.57	4.1E-04	3.4E-04	1.9E-04	1.4E-04	1.8	2.4	1.3
6:1	10	0.1 M	1.2	7.2E-04	6.7E-04	1.9E-04	6.1E-05	3.5	11	3.1
6:2	10	0.1 M	1.2	8.4E-04	7.8E-04	2.3E-04	6.1E-05	3.4	13	3.7
6:3	10	0.1 M	1.1	5.1E-04	4.7E-04	2.0E-04	6.1E-05	2.3	7.6	3.3
7:1	10	0.05 M	0.58	5.3E-04	4.4E-04	1.3E-04	2.6E-05	3.3	17	5.1
7:2	10	0.05 M	0.58	5.8E-04	4.9E-04	1.8E-04	2.6E-05	2.8	19	6.8
8:2	10	0.1 M	1.1	2.0E-04	1.8E-04	2.4E-05	2.4E-05	7.5	7.4	1.0
8:3	10	0.1 M	1.1	2.6E-04	2.2E-04	2.5E-05	2.4E-05	9.1	9.4	1.0
9:1	10	0.05 M	0.57	5.0E-04	4.2E-04	7.1E-05	4.5E-05	5.9	9.3	1.6
9:2	10	0.05 M	0.58	5.6E-04	4.7E-04	1.1E-04	4.5E-05	4.2	11	2.5
9:3	10	0.05 M	0.64	4.1E-04	3.4E-04	9.4E-05	4.5E-05	3.6	7.6	2.1
AD-1	12	0.05 M	0.59	6.1E-04	5.2E-04	2.3E-04	2.3E-04	2.3	2.2	1.0
AD-3	11	0.05 M	0.59	5.7E-04	4.8E-04	1.8E-04	2.0E-04	2.7	2.5	0.92
AD-31	33	0.05 M	0.59	6.5E-04	5.6E-04	1.3E-04	1.4E-04	4.3	4.1	1.0
358.87	16	1.0 M	7.5	2.0E-04	2.0E-04	7.6E-05	7.5E-05	2.6	2.6	1.0
358.94	121	1.0 M	7.5	2.1E-04	2.1E-04	8.7E-05		2.4		
372.84	15	0.5 M NaHCO3				2.2E-04				
378.13	15	0.1 M KCl	1.2	3.2E-04	2.9E-04	1.6E-04	1.8E-04	1.8	1.6	0.89
739.9	46	1.0 M	7.5	5.5E-04	5.4E-04	3.2E-04		1.7		
746.59	106	1.0 M	7.5	2.2E-04	2.2E-04	1.6E-04		1.3		
746.65	15	1.0 M	7.5	2.4E-04	2.4E-04	9.1E-05	1.5E-04	2.6	1.6	0.61
755.49	15	1.0 M	7.5	1.6E-05	1.4E-05	3.7E-06		3.9		
765.53	98	1.0 M	7.5	1.6E-04	1.6E-04	8.2E-05		1.9		

Notes to tabulated data in Appendix B

- **Samples 1:2 (0.05) to 9:3** from Löfgren et al. (2009, Appendices A8-A9, B). Labelling according to sample number:experimental run (electrolyte concentration).
- **Samples AD-1 to AD-31** from Vecernik et al. (2012, Tables 1 and 3). TD effective diffusivity recalculated to TD F_f by using $D_w = 2 \cdot 10^{-9}$ m^2/s (Vecernik et al. 2012, p 143 and Equation 6). Pore water EC not stated in article. It was estimated by taking the arithmetic mean of all EC pore water data for sample/run 1:2, 3:1, 3:2, 5:1, 5:2, 7:1, 7:2, 9:1, 9:2, and 9:3.
- **Samples from 358.87 to 765.53** from Löfgren and Neretnieks (2006, Tables 1 and 2). Corresponding pore water EC = 7.5 S/m from Löfgren (2004, Section 4.1.5) and of 1.2 S/m estimated from standard values at room temperature for the KCl solution.
- In the above references (Löfgren and Neretnieks 2006, Löfgren et al. 2009, Vecernik et al. 2012) the apparent formation factor was reported from direct current measurements. By using the apparent formation factors and pore water ECs, as tabulated above, and Equation 6-29 of SKB (2010a), the DC formation factor could be calculated.